ISTANBUL TECHNICAL UNIVERSITY ★ GRADUATE SCHOOL OF SCIENCE ENGINEERING AND TECHNOLOGY

HOMOGENIZATION OF ADDITIVELY MANUFACTURED POLYMERIC FOAMS WITH SPHERICAL CELLS

M.Sc. THESIS

Hamed ZEINALABEDINI

Department of Mechanical Engineering

Machine Design Program

MAY 2015

ISTANBUL TECHNICAL UNIVERSITY ★ GRADUATE SCHOOL OF SCIENCE ENGINEERING AND TECHNOLOGY

HOMOGENIZATION OF ADDITIVELY MANUFACTURED POLYMERIC FOAMS WITH SPHERICAL CELLS

M.Sc. THESIS

Hamed ZEINALABEDINI
503121231

Department of Mechanical Engineering

Machine Design Program

Thesis Advisor: Asst. Prof. Dr. Mesut Kırca

MAY 2015

İSTANBUL TEKNİK ÜNİVERSİTESİ ★ FEN BİLİMLERİ ENSTİTÜSÜ

KATMANLI ÜRETİMLE ÜRETİLEN KÜRESEL HÜCRE YAPILI POLİMERİK KÖPÜKLERİN HOMOJENLEŞTİRİLMESİ

YÜKSEK LİSANS TEZİ

Hamed ZEINALABEDINI
503121231

Makine Mühendisliği Anabilim Dalı

Konstrüksiyon Programı

Tez Danışmanı: Yrd. Doç. Dr. Mesut Kırca

MAYIS 2015

Hamed Zeinalabedini, a **M.Sc. student of ITU Graduate School of Science Engineering and Technology** student ID **503121231**, successfully defended the **thesis** entitled "**HOMOGENIZATION OF ADDITIVELY MANUFACTURED POLYMERIC FOAMS WITH SPHERICAL CELLS**", which he prepared after fulfilling the requirements specified in the associated legislations, before the jury whose signatures are below.

Thesis Advisor:	**Asst. Prof. Dr. Mesut Kırca** Istanbul Technical University	....
Jury Members:	**Prof. Dr. Vedat Ziya Doğan** Istanbul Technical University	....
	Asst. Prof. Dr. Atakan Altınkaynak Istanbul Technical University	....

Date of Submission: 03 May 2015
Date of Defense: 05 June 2015

To my family,

FOREWORD

It is a humbling experience to acknowledge those people who have, mostly out of kindness, helped me along the journey of my Master. I am indebted to so many for their encouragement and support.
My sincerest thanks are extended to my project supervisor and mentor, Asst. Prof. Dr. Mesut Kirca, for his encouragement and guidance.
To my family, you should know that your support and encouragement meant more than I can express on paper.

June 2015 — Hamed Zeinalabedini
(Mechanical Engineer)

TABLE OF CONTENTS

Page

LIST OF TABLES

Page

LIST OF FIGURES

Page

OMOGENIZATION OF ADDITIVELY MANUFACTURED POLYMERIC FOAMS WITH SPHERICAL CELLS

SUMMARY

Exciting progress in additive manufacturing (AM) technology, which enables fabrication of cellular structures such as highly complex lattice and porous structures, has stimulated the development of lightweight structural products with improved performance and increased functionality. However, conventional design and analysis tools lack the ability to optimize complex geometries efficiently and robustly. With this motivation, in this study, homogenized material models of open-cell polymeric foams with spherical cell architectures that are manufactured using AM technology are formulated through both experimental and numerical investigations, which in turn can be employed in a novel micromechanics based topology optimization algorithm [1] developed for the optimization of cellular structures. In this regard, for the purpose of generating computer aided drawing (CAD) data, which is mandatory for AM, randomly intersected spherical ensemble method [2] is employed. Several foam models with different porosities are generated and utilized in nonlinear finite element analyses (FEAs) to determine constitutive elastic constants. Plastic stress-strain data for the bulk AM material are obtained through static tensile tests in different loading directions and used in FEA as true stress-strain data. Homogenization is performed based on a quadratic form of the widely used Gibson and Ashby foam model that describes the Young's modulus E^*, and yield strength σ^*_{pl} of cellular structures in terms of relative density. Coefficients of the quadratic scaling laws are fitted by both FEA and experiments which are compared with each other.

KATMANLI ÜRETİMLE ÜRETİLEN KÜRESEL HÜCRE YAPILI POLİMERİK KÖPÜKLERİN HOMOJENLEŞTİRİLMESİ

ÖZET

Son derece karmaşık kafes ve gözenekli yapılar gibi hücresel yapıların imalatına olanak tanıyan katmanlı üretim teknolojisi (KÜT); gelişmiş performans ve artan işlevselliği ile hafif, yapısal ürünlerin geliştirilmesini teşvik etmektedir. Fakat, geleneksel tasarım ve analiz araçları kompleks geometrilerin verimli ve düzgün bir şekilde optimize edilmesine olanak tanımaz. Bu noktadan cıkışla, bu çalışmada, KÜT ile üretilmiş küresel ve açık hücre yapılı polimerik köpüklerin homojenize malzeme modelleri sayısal olarak gerçekleştirilmiştir ve deneysel sonuçlarla karşılaştırılmıştır. Hücresel yapıların optimizasyonu için yakın zamanda geliştirilen bir topoloji optimizasyon yönteminde kullanılabilecek mikromekanik modeller geliştirilmiştir [1]. Bu bağlamda, KÜT için zorunlu olan bilgisayar destekli çizimlerini (CAD) oluşturmak amacıyla rastgele kesişen küresel topluluk yöntemi kullanılmıştır [2]. Farklı boşluk oranlarına sahip 5 farklı köpük modelinin; yapısal elastik sabitlerini belirlemek için lineer olmayan sonlu eleman analizleri gerçekleştirilmiştir. Katmanlı üretimle üretilen yığın malzemeler için plastik gerilme-birim uzama verileri, farklı yükleme yönlerindeki statik gerilme testleri ile elde edilmiş ve sonlu eleman analizlerinde doğru gerilme-uzama verisi olarak kullanılmıştır. Homojenleştirme; Young modülü E^*, ve akma mukavemeti σ^*_{pl} parametreleri için, Gibson-Ashby köpük modeline bağlı olarak, bağıl yoğunluğun bağımsız değişken olarak kullanıldığı ikinci mertebeden fonksiyonların katsayılarının belirlenmesi ile gerçekleştirilmiştir. Sayısal testler ile gerçekleştirilen homojenleştirme ve deneysel sonuçlar ile gerçekleştirilmiş homojenleştirme, ilgili ikinci mertebeden fonksiyonların karşılaştırılması suretiyle değerlendirilmiştir.

1. INTRODUCTION

Cellular materials have received a considerable amount of attention in recent years because of their combined physical and mechanical functional properties, such as low density, their high mechanical energy absorption efficiency, and their damping capacity. There are several methods for the manufacturing of cellular materials. Recently with developing the additive manufacturing method with a capacity to produce complex geometry, it is possible to manufacture highly porous cellular materials. Additive manufacturing processes allow us to create complex shapes without requiring expensive or many different tools. In fact, additive manufacturing will be a conventional method playing a dominant role in contemporary cellular structure production. In order to obtain variable density additive manufacturing cellular structure, it is important to establish a design optimization method for additive manufacturing (Mun, Yun, Ju, & Chang, 2015). In the literature, for optimize and accuracy for the design process of relative density or porosity of cellular structure during additive manufacturing mainly employs three key techniques: homogenization, optimization, and construction.

This thesis concerns the homogenization of the polymer basic cellular highly porous produce in additive manufacturing as a first step of the optimize design process of porosity and relative density during additive manufacturing. The first chapter including the introduction of major topic discussion in this thesis. The other major is the technique involved in the thesis. At the end of the introduction the thesis plane explains. The second chapter is the material modeling. The process which improves the material properties of foams explained. To improve the material properties the composite models applied.

The third and fourth chapter, homogenization of randomly organized polymeric foams has been studied by employing finite element method. For this purpose, CAD models of the foams with varied porosities are prepared through a quasi-stochastic process and numerical specimens are generated by commercial finite element software. Finite element analyses which are taking into account nonlinear geometrical effects and nonlinear material properties are performed to exploit the compressive mechanical behavior of the foams. Gibson-Ashby homogenization model has been utilized for the homogenization of polymeric cellular solids. In chapter five numerical results are compared with the experimental results to provide the degree of reliability of the finite element simulations.

1.1 Additive Manufacturing

Additive manufacturing is a layer basic technology, which composes 3-diminsional objects using a scaled physical facsimile of the 3-dimensional CAD date set (solid) (Gebhardt, 2012).The key how AM works is that; parts are made by adding material in layers; each layer is a thin cross-section of the part derived from the original CAD data.

AM is a variety of different manufacturing processes that requires no individual tooling. Although, AM machine-related processes are capable of processing a wide variety of materials. Beside plastic, metal and ceramic materials which are frequently used in industry are capable of being processed by AM machines. Car companies, aerospace, toy industries, medicine, etc., use AM, not only because of the variety of materials, but also to bring new ideas to reality, with limitless shape geometry (Gebhardt, 2012).

While using AM you can produce complex shapes at the macro or micro level, without reducing the speed of production. (Klahn, Leutenecker, & Meboldt, 2014). For end-user products, individual parts as well as series products, higher durability and long term stability are required. Despite the fact that AM is an expensive operation, at the end it costs beneficial, since it requires less time and tools, workers, space, and other elements during manufacturing. It has been under development for at least three decades, AM has recently received extraordinary public attention (Klahn, Leutenecker, & Meboldt, 2014).

The most common additive manufacturing processes are photo polymerization processes, powder bed fusion processes, and extrusion-based (Gibson, Rosen, & Stucker, 2010). Photo polymerization systems use of liquid radiation curable resins or photopolymers as their primary materials. Most photo polymers react to radiation in the ultraviolet (UV) range of wave lengths, but some visible light system are used as well. Powder bed fusion processes (PBF) were among the first commercialized AM processes. Developed at the University of Texas at Austin, USA. Selective laser sintering (SLS) (J. Munguia, 2014)was the first commercialized powder bed fusion process, shown in Figure 1. Its basic method of operation is schematically shown in Figure 1 and all other PBF processes modify this basic approach in one or more ways to enhance machine productivity, enable different materials to be processed, and/or to avoid specific patented features.

Extrusion-based systems use extrusion to form parts. These technologies can be visualized as similar to cake icing, in that material contained in a reservoir is forced out through a nozzle when pressure is applied (Stucker, 2010). If the pressure remains constant then the resulting extruded material flow at a constant rate and remain a constant cross-sectional diameter. This diameter will remain constant if the travel of nozzle across a depositing surface is also kept at a constant speed that corresponds to the flow rate. The material that is being extruded must fully solidify while remaining in the shape. Furthermore, the material must bond to material that has already been extruded so that a solid structure can result.

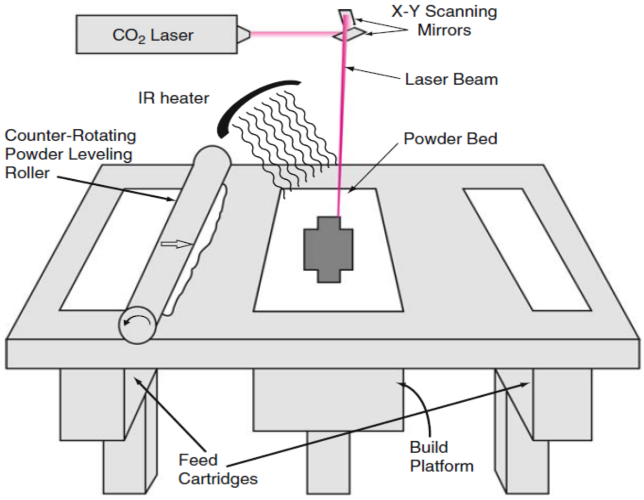

Figure 1: Schematic of the selective laser sintering process

There are some of key features that are usually used to any extrusion-based system, loading of material, liquefaction of the material, application of pressure to move the material through the nozzle, extrusion, plotting according to a predefined path and in a controlled manner, bonding of the material to itself or secondary build materials to form a coherent solid structure, inclusion of support structures to enable complex geometrical features.

Solid free form fabrication (SFF) technologies in general have the ability to manufacture functional parts with locally controlled properties. In fact, that provides an opportunity for manufacturing a whole new class of products.

Fused deposition modeling (FDM) (S.-M. Ahn, 2002) is covered by SFF technology and the extrusion based system. FDM has the potential to produce parts with locally controlled properties. FDM processes fabricate by extruding a semi molten filament through a heated nozzle in a prescribed pattern onto a platform layer by layer, as shown in Figure2.

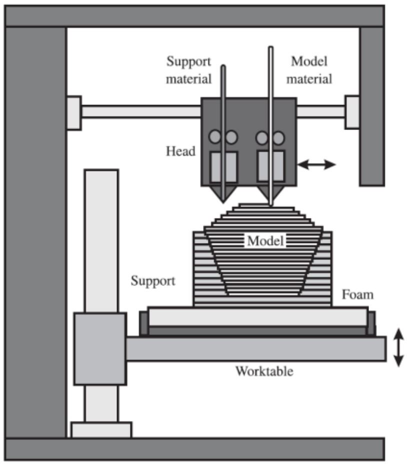

Figure 2: Schematic Diagram of FDM Process

FDM processes use several types of material, such as acrylonitrile-buta-diene-styrene (ABS) and investment casting wax.

1.2 Cellular Materials

The cellular materials are the basic of study in the thesis. Natural materials, such as wood, cork and cancellous bone, and man-made materials such as honeycombs and foams, are well known example of cellular solids. Common to all of them is a microstructure consisting of an interconnected network of struts (open cells) or plates (closed cells) (N. Michailidis, 2010).

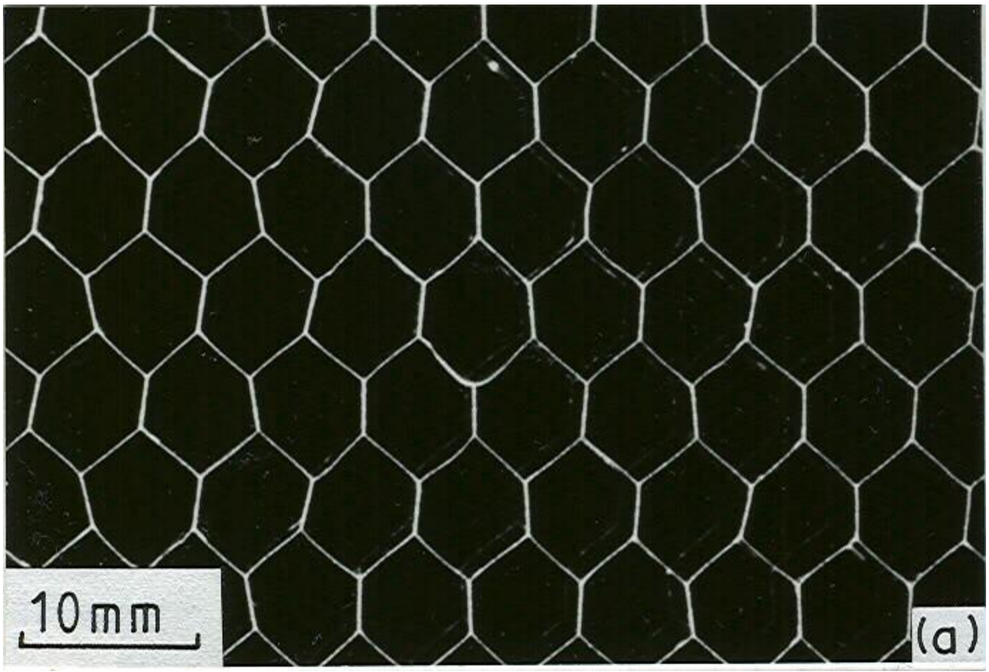

Figure 3: Engineering cellular solids: aluminum honeycomb

Cellular materials with phenomenal properties such as low density, high mechanical energy absorption efficiency, damping capacity, and novel physical such as thermal, electrical and acoustic properties are used widely in engineering (Goodall & Mortensen, 2014). In order to describe the properties of cellular materials, we depend on the relative density, relative elastic modulus, etc., (F.Ashby, et al., 2000). The Mechanical properties of cellular materials do not depend only on properties of the materials of which the ligaments are made, but also on the micro-morphology, i.e. the spatial distribution of cells (e.g. size, shape, etc.) (Nguyen & Noels, 2014).

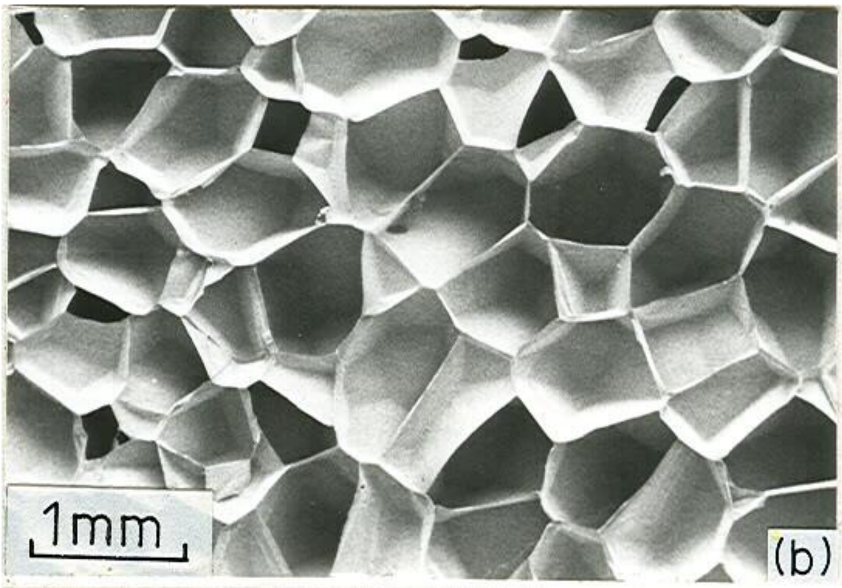

Figure 4: open-cell polyurethane foam

Cellular materials are extremely attractive option to produce stiff materials with low weight (Michailidis, 2011). Polymeric, ceramic, or metallic foams are either used or considered for a variety of applications ranging from light weight structures to packing insulation or crash protection (S.K. Nammi, 2010). For a mechanical viewpoint, the primary quantity controlling the properties is the relative density ρ*/ρ where ρ* is the density of the cellular material and ρ the density of the corresponding bulk. Foams, the elastic modulus E*, during initial loading appears to be elastic, but the initial loading curve is not straight, and its slop is less than the true modulus, because some cells yield at very low loads (Zi-Xing Lu, 2011). The real modulus is best measured dynamically or by loading the foam into the plastic range, then unloading the determining E from the unloading slope. Young's modulus, E scales with density:

$$\frac{E^*}{E_s} = \boldsymbol{C}_1(\frac{\rho^*}{\rho_s})^n \qquad (1)$$

Where n has a value between 1.8 and 2.2 and C_1between 0.1 and 4 – they depend on the structure of the metal foam.

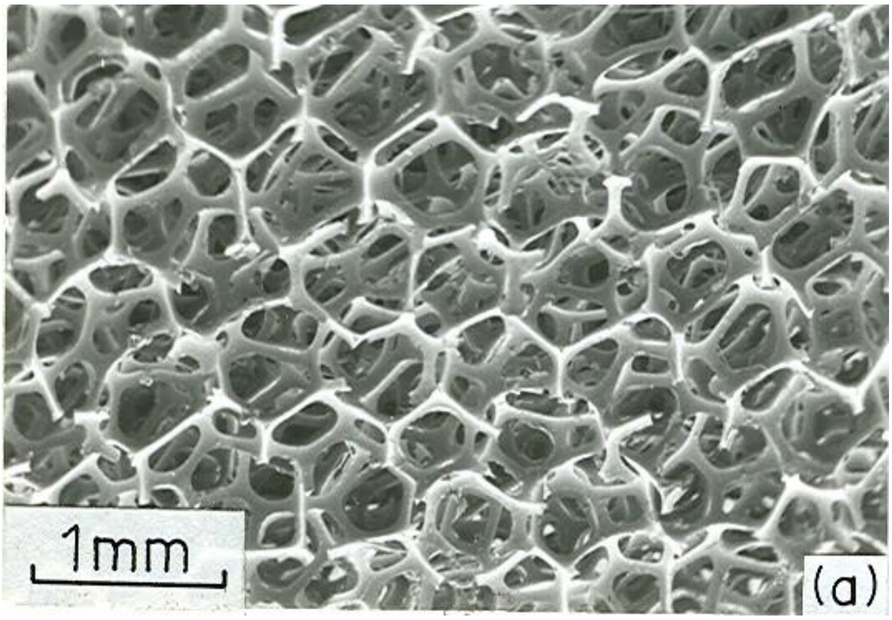

Figure 5: closed-cell polyethylene foam

Former manufacturing of cellular materials have had several methods: mix metal powders with a blowing agent, bubbling gas in liquid, injection of gas directly into the molten, etc. (Tapan Sabuwala, 2013). For these methods the random shape and ligament are created. The only factor that has control on the cellular properties are the main material mechanical properties (R.K. Oruganti, 2008). Using these methods, cellular properties can be controlled by the original material properties. The cell's structure, such as shape, ligament thickness, and cell distributions are not able to be controlled by us (Mun, Yun, Ju, & Chang, 2015). Actually this random distribution may result in recognizably different mechanical properties (Beckmann & Hohe, 2014). The AM available technologies directly fabricate 3D cellular structures. In spite of the fact of AM's susceptibility fabricate parts with complex cellular geometry, it still needs scalability to cover more materials.

It is important to individualize between the properties of the cellular materials and those of the solid from which it is made (Jane Chu, 2010).The attempts for modeling the mechanical properties of cellular materials presents the relative elastic modulus and relative yield stress of highly cellular materials as a function of the relative density (F.Ashby, et al., 2000). A mixture of cell shape and material properties building the material gives us manual properties of mechanical behavior and the considerably low ratio of weight to strength. Further, researchers' investment of efforts in the analysis of microstructure-strength relationships of cellular materials, seeking the recipes for optimal design of materials and construction brings opportunity for multifunctional performance (Niu, Yan, & Cheng, 2008).

1.3 Structural Optimization of Lattice Structures

With the appreciable progress in additive manufacturing technology, complex shaped lattice structures can be easily manufactured providing the construction of lightweight structures. In this regard, new optimization schemes need to be developed to efficiently carry out structural optimization of lattice structures that will be manufactured by AM methods. In this section, one of those optimization schemes that have been developed recently for the optimization of cellular materials will be introduced and the relation between this thesis studies with the mentioned optimization method will be explained.

The purpose of the design optimization scheme is to establish an efficient computational method to optimize the topology of load-bearing cellular structures manufactured by AM. It is known that AM has influenced multiple fields, such as prototype manufacture, material design, and biomedical engineering. It has been mentioned that AM can readily manufactures cellular structures with complex cell, geometry and variable density, in fact this technique affects the design, optimization, and manufacture of load bearing cellular structure with variable density. However, some improvements and developments on the AM technique are required for designing and manufacturing uniform density or stochastic cellular structures.

AM offers several important advantages in structural product design using variable-density cellular structures:

i. Allow mechanical properties to be varied spatially
ii. Reduce amount of used material
iii. Reduce energy consumption in weight-sensitive applications
iv. Increase resistance and tolerance against defect generations

To be able to utilize variable-density AM cellular structures, a design optimization method has one main rule for producing optimum cellular structures. To establish a design optimization method for AM, since much work has already been done on topology optimization of a single unite cell of cellular lattice structures, there are two main topology optimization methods. The first method optimizes the density distribution of the solid material block, and then remaps the material density to a typical cellular structure. The second one designs the lattice and cell structure beforehand and then optimizes the strut size or wall thickness within one cell.

The concern of this thesis is a study on the first approach for optimizing porosity of cellular structure during the additive manufacturing. This method has efficiency in rapid design and analysis (Mun, Yun, Ju, & Chang, 2015).

1.3.1 Design method

The design methodology involves in this thesis is based on establishing an efficient computational method to optimize the topology of load-bearing cellular structures manufactured by AM.

The design process mainly employs three key techniques:

i. Homogenization
ii. Optimization
iii. Construction

The literature calls these three techniques HOC (**H**omogenization, **O**ptimization, **C**onstruction). This HOC method gains efficiency by avoiding topology optimization on close cellular structures, yet maintains accuracy and reliability through developing suitable micromechanics models.

The homogenized step, Figure 6(a), uses an equivalent continuous solid to represent a cellular structure by introducing a homogenization material constitutive law, which is a function of the cellular structure's microstructure characterizing parameters (MCPs), such as relative density and cell orientation. For regular cellular structure, designers are able to define the MCPs related constitutive law from computational micro-mechanics models or experimental tests. Using well-developed continuum for directing the outcome of the first step can be optimized rapidly with topology optimization theory, shown in Figure 6(b). Thus, the optimized MCP (average density …) distribution is obtained, shown in Figure 6(c). Finally, the detailed cellular structure is constructed explicitly by mapping the obtained MCP distribution into individual cells.

Regarding the HOC, in this thesis the homogenization of cellular structure is studied. For optimization, the homogenization polymer base of cellular structure is utilized.

The output of this thesis can optimize the design and specifies the density mass scattering.

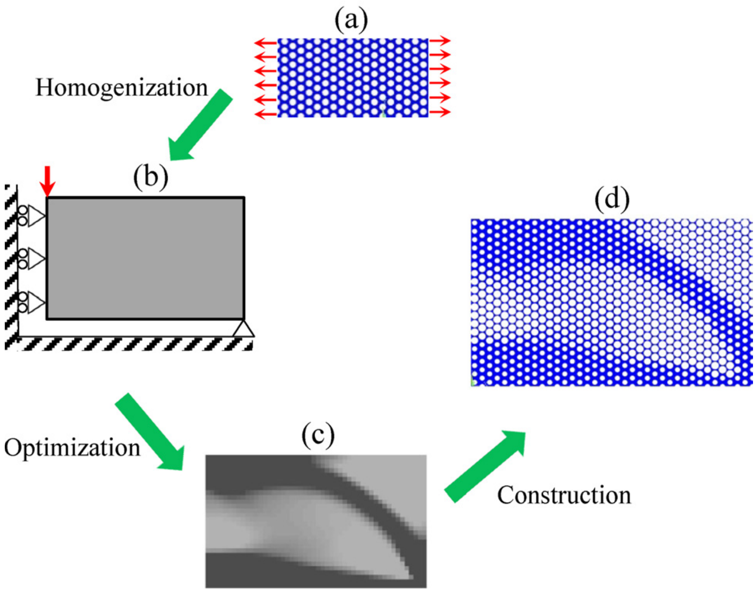

Figure 6: Steps of schematic illustration of the HOC during the design-optimization process of an AM cellular structure: (a) material property modeling based on the computational micromechanics model. (b) Continuous solid model based on obtained homogenized material properties. (c) Topology optimization for the continuous solid model (dark gray scales indicate higher local density of material). (d) Explicit cellular structure obtained from cell construction step.

1.4 Homogenization of Cellular Materials

The main goal of this study is to reach homogenization models of the randomly structured polymeric foams which in turn can be used in the HOC optimization process explained above. According to that, the results obtained through this thesis can be utilized to manufacture optimized foam geometries by using AM technology. In literature, the variety of methods such as probabilistic homogenization (Beckmann & Hohe, 2014), experimental and finite element analysis (FEA) (Szymczyk & Miedzińska, 2010) (Michailidis, Stergiudi, Omar, Papadopoulos, & Tsipas, 2011) have been developed to calculate the effective mechanical properties. As one of these methods, the Voronoi tessellation technique based on the three-scale finite element method predicts the effective properties of periodic materials (K, X, & Subhash, 2005). Subhash and Li have used some foam samples based on Voronoi diagrams, which are constructed by FE models. Study of them show that the strut cross-sectional shape is worthy of attention and important. Michailidis and Stergioudi (Michailidis, Stergioudi, Omar, Papadopoulos, & Tsipas, 2010) also studied about experimental and FE analysis of the cellular material properties, which has shown that the distributions of local stresses and strains can be different with size, orientation and spatial arrangement of the cellular. The study of Beckmann and Hohe to predict the mechanical properties of solid foams employs the numerical homogenization analysis of small-scale testing volume elements (Beckmann & Hohe, 2014). For the numerical homogenization, they utilize a finite element technique. The study shows that the numerical prediction of the elastic modulus based on the known uncertainty of the local relative density for aluminum foam provides a good approximation of the experimental result. (Beckmann & Hohe, 2014)

By the significant progress in AM technology, now wide variety of industrial materials can be used to manufacture complex shaped products. Consequently, development of efficient and robust techniques for the optimization of complex shaped parts is currently under investigation by several research groups. As introduced in previous section, HOC is one of the most recent optimization schemes developed for the cellular lattice structures. In the first step of this optimization process, cellular structures are associated to the continuum model based on homogenized material properties (Pu Zhang, et al., 2015).

Conventional cellular structures can be named as open cell (cells joint by struts) or closed cell (enclosed by faces) depending on the inter-connectivity of cells. Their mechanical properties according to Gibson-Ashby model (F.Ashby, et al., 2000) depend on the constituent material, the relative density. The Young's modulus E, shear modulus G, and yield strength σ_plof the cellular structures have polynomial law relationships, with respect to relative density ρ(x). For example quadratic law is general used for elastic modulus, also it is usually utilized from FEA or experimental result. Using additive manufacture gives the ability to change the cellular structures such as ligament and porous spatial distribution, and the even more complex cellular structure, the scaling low for material properties should be more complicated. In general, the cellular structures behave more like anisotropic instead of isotropic. There is a study show that for the anisotropic constitutive law

$$\sigma = \mathbf{C}\varepsilon \qquad (2)$$

is used, where σ, **C**, and ε are the stress, elastic matrix, and strain, respectively (Mun, Yun, Ju, & Chang, 2015). For a plan stress problem we have,

$$\sigma = [\sigma_1 \sigma_2 \sigma_3]^T \qquad (3)$$

$$\varepsilon = [\varepsilon_1 \varepsilon_2 \varepsilon_3]^T$$

$$C = \begin{bmatrix} C_{11} & C_{12} & C_{13} \\ C_{21} & C_{22} & C_{23} \\ C_{31} & C_{32} & C_{33} \end{bmatrix}$$

Where the subscript 1 and 2 indicate horizontal and vertical direction, respectively; σ, ε, τ and γ are the normal stress, normal strain, shear stress, and shear strain, respectively.

The study show a polynomial function that can be fit the scaling laws. In case of only one MCP, for example, relative density ρ(x), the elastic matrix of cellular structures can be written as

$$\mathbf{C}(\rho) = \mathbf{C}_0 + \mathbf{C}_1\rho + \mathbf{C}_2\rho^2 + \cdots \qquad (4)$$

Where $\mathbf{C}_i (i = 0, 1, 2, \ldots)$ are constant symmetric matrices to be determined from the computation or experimental result. Equation (4) is for generalized anisotropic case. With simplified the equation (4) it can be used for isotropic or orthotropic cases (Mun, Yun, Ju, & Chang, 2015).utilized the symmetric condition reduce the number of parameters can be fitted, , it can act as advantage to simplified the calculation. Equation (4) would defined on mechanical properties, such as yield strength and thermal expansion rate.

1.5 Purpose of the Study

The objective of this work is to establish an efficient computational method for the homogenization (as a first step of computational design) of load-bearing cellular structures manufactured by AM. As a first step of purpose of this study, the CAD data for the randomly structured open cellular solids with spherical cells were generated. The steps of this generation start with defining the coordinate of random point with numerical software, MATLAB. These point as a script add to the CAD modeling software. The next step, illustrate preparation of FE models for the foam structures which have different porosities. To solve nonlinear FE models, static analysis applied, Figure 7. To be confident about the FE analysis result, the 3D models of cellular structures extracting with the partner form Pittsburgh University. The tensile and compression tests were performed by our US partner.

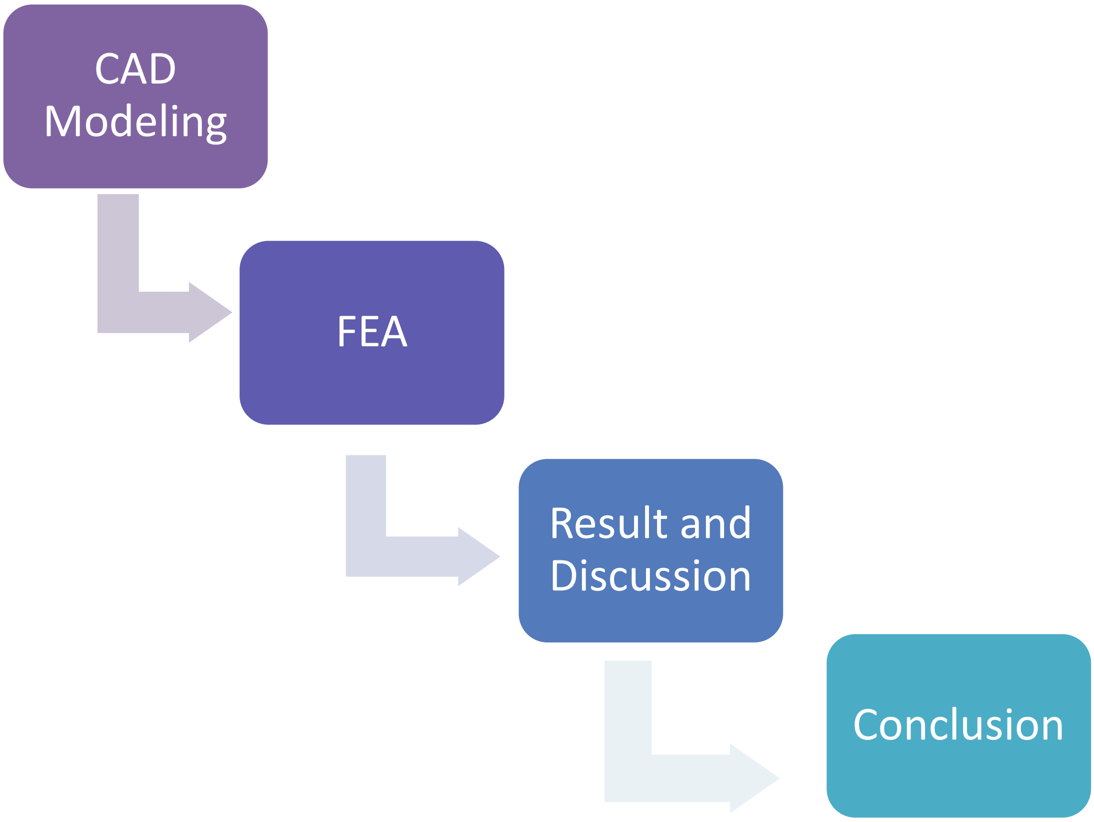

Figure 7: Plan of study

In this study it is applied Gibson-Ashby technique by using the nonlinear finite element and experimental methods for homogenization. It explained the procedure of defining CAD modules and AM manufacturing, and will illustrate how the finite element and experimental methods are involved, and discuss the results. In our study choosing common polymer Vero white, which is used in a wide range of industrial and medical instrument. To analyze the module in this study we used the finite element analyzer software. In order to define the material properties ,used the plastic-elastic module with Isotropic, Kinematic hardening, each one of which showed us different kinds of behavior; in order to improve the results simulation of compression bulk material by using the tension test results. For this simulation employed composite property for compression and tension tests. For the experimental method we used the Vero white sample, which was printed by the Fusion Deposition Method (FDM).

2. NUMERICAL MODELING OF CELLULAR STRUCTURE

Additive manufacturing gives opportunity to produce complex geometry without increased product cost. Even at the micro and macro scale you can design and product the variance of structure. AM technology produces a variety of shapes and dimensions of cells and porous. In our study we produced the cellular structure using spherical topology. The fundamentals of understanding the definition of spherical cells being used require solid isotropicmaterial with penalization algorithm (Bendsøe, M. P., & Sigmund, 1999). The CAD (Computer Aided Design) software technology develops very fast and become an indispensable part of the engineering application. Design and create more complex 2D and 3D geometry utilized faster and easily. Also the accuracy of the design get higher and manufacture costing less money and cheaper.

2.1 Computer Aided Design for Spherical Cells

The models of the cellular structure are more complex. For simulation of non-uniform cellular structure with spherical cells, we are developed algorithm at numerical analysis program MATLAB, which it generates random points and forms an structure using these points coordinates. To understand how the distribution of spherical cells can affect the mechanical properties, five different models are defined, with variety of different relative density. According to the Ashby and Gibson model (F.Ashby, et al., 2000), the elastic modulus E, yield stress σ_{pl} of cellular structure have polynomial law relationships with respect to the relative density $\rho(x)$.

For each models the random scattering of the point satisfied the porous ligament thickness and approach target density for each models individually. Modeling capability for products to be designed plays an important role in order to effectively construct and utilize CAD/CAM system. For modeling and simulated of cells structure used CAD CAM software. The random interconnected spheres are shown in Figure 8. The finial random foam with 0.4, 0.35, 0.3, 0.25, and 0.20 relative density shown in Figure 9, 10, 11, 12, and 13, respectively.

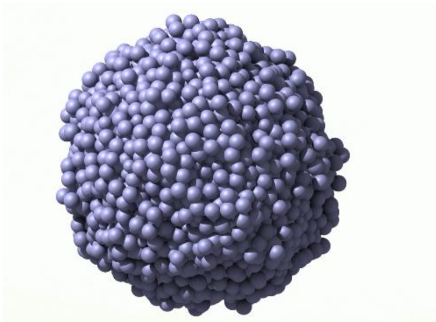

Figure 8: Random interconnected spheres

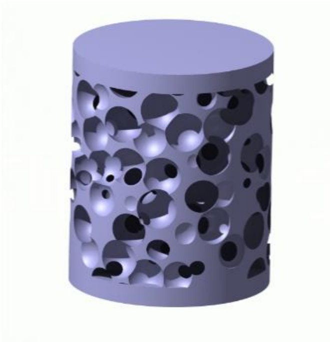

Figure 9: Final cellular structure with 0.4 relative density block after extraction

Figure 10: Final cellular structure with 0.35 relative density block after extraction

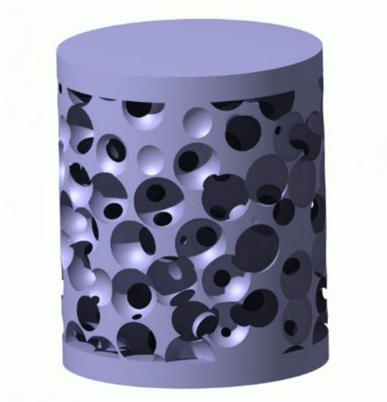

Figure 11: Final cellular structure with 0.3 relative density block after extraction

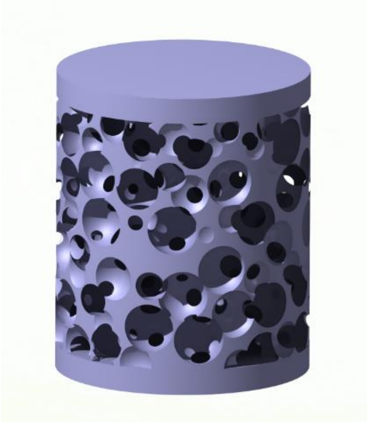

Figure 12: Final cellular structure with 0.25 relative density block after extraction

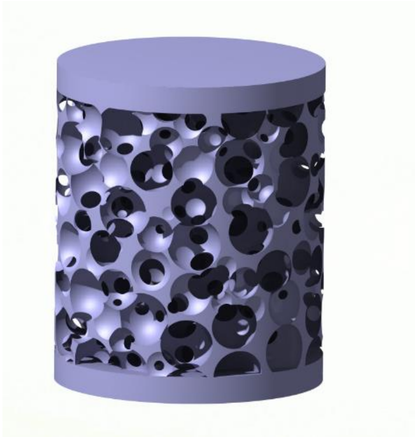

Figure 13: Final cellular structure with 0.2 relative density block after extraction

2.2 Finite Element Modeling of Cellular Structures

2.2.1 Meshing and finite element properties

The material properties described above were selected. From the bulk model, the compression test results were used to define Young's models. The nominal stress and

Nominal strain converted into true stress and true plastic strain in order to be input into the FEA software. Young’s model is 1659.9 MPa and Poisson ration selected 0.39 from literature (Li, Sun, Bellehumeur, & Gu, 2002). The element types 15-node quadratic triangular prism and 10-node quadratic tetrahedron are in the list of continuum, structural, and rigid body elements utilized for meshing the foams, the table 2 shows the mesh properties. The definition of rigid body specifies the region of the model containing all of the elements that are part of rigid body. Elements in this region or nodes which are connected to the elements in this region cannot be part of any other rigid body also element type 15-node quadratic triangular prism has ability to convert automatically to the corresponding variable, if it has faces that are part of the slave surface in a node-to-surface contact pair. Element type 10-node quadratic tetrahedron and 15-node quadratic triangular prism are three dimensional solid elements available. The element type 10-node quadratic tetrahedronhas 10-node quadratic tetrahedron, and element type 15-node quadratic triangular prism has 15-node quadratic triangular prism. The element type’s 15-node quadratic triangular prism choice for support meshing and Element types 10-node quadratic tetrahedron choice for foams meshing.

Table 1: Mesh properties of FEA models

Relative density	Number of element type 15-node quadratic triangular prism	Number of element Type 10-node quadratic tetrahedron	Total elements number
0.40	129654	1027048	1156702
0.35	129654	925320	1054974
0.30	130704	874587	1005298
0.25	131978	776038	908016
0.2	64928	865555	930483

The element types 10-node quadratic tetrahedronare geometrically versatile and are used in many automatic meshing algorithms. It is very convenient to mesh a complex shape, in fact, because of tetrahedral and second order ability. However, a good mesh of 10-node quadratic tetrahedron elements usually provides a solution of equivalent accuracy at less cost. The 10-node quadratic tetrahedron elements have a good convergence rate, and sensitivity to mesh orientation in regular meshes is not an issue. The finite element commercial software manual recommended if an automatic tetrahedral mesh generator is used second order elements 10-node quadratic tetrahedron in analyses with large amounts of plastic deformation. The mesh of foams with relative density 0.4, 0.35, 0.3, 0.25, 0.2 are shown in Figure 14, 15, 16, 17, and 18, respectively.

Figure 14: Cellular structure with 0.4 relative density block meshing

Figure 15: Cellular structure with 0.35 relative density block meshing

Figure 16: Cellular structure with 0.3 relative density block meshing

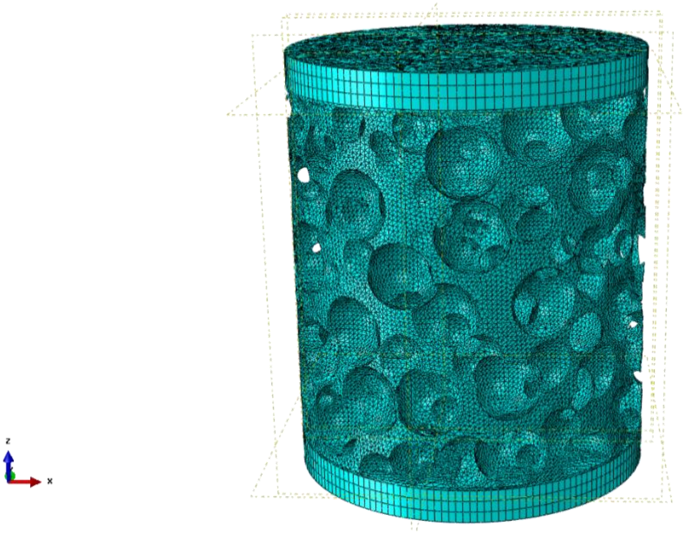

Figure 17: Cellular structure with 0.25 relative density block meshing

Figure 18: Cellular structure with 0.2 relative density block meshing

2.2.2 Nonlinear finite element modeling

The objective of the analysis is to determine static response during large deformation. In a nonlinear analysis, the solution cannot be calculated by solving a single system on linear equations, as would be done in linear problem. Instead, the solution is found by specifying the loading as a function of time and incrementing time to obtain the nonlinear response. Therefore, FEA software breaks the simulation into a number of time increments and finds the approximate equilibrium configuration at the end of each time increment. For the body to be in equilibrium, the net force acting at every node must be zero. Therefore, the nonlinear response of a structure to a small load increment ΔP, is shown in Figure 19, which with uses the structure's tangent stiffness, K_0 which is based in its configuration atu_0, and ΔP to calculate a displacement correction,c_a for the structure. Using c_a, the structure's configurations is updated to u_a.

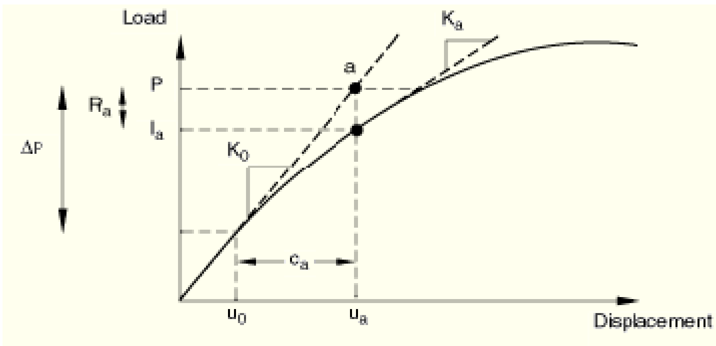

Figure 19: First iteration in an increment

As described above, and then calculates the structures internal forces,I_a in this new configuration. The difference between the total applied load, P and I_a can now be calculated as

$$\mathrm{P} - I_a = \mathrm{R_a} \tag{5}$$

where, $\mathrm{R_a}$ is the force residual for the iteration.

2.2.2.1 Large deformation

In non-linear static finite element analysis involving large displacements, large strains and material nonlinearities, it is necessary to resort to an incremental formulation of the equations to described the affection. To provide general analysis, which can capable for a general formulation, need to have isoperimetric finite element.

Two approaches have been pursued in incremental nonlinear FEA. The main different of this approaches are for static variables are referred to an updated configuration in each load step. This procedure is mostly called Eulerian, moving coordinate or updated formulation. Meanwhile, in the second approach, which is generally called Lagrangian formulation, all static and kinematic variables are referred to the initial configuration (KLAUS-JURGEN, 1975).

Whether the displacement, or strain, are large or small, it is vitally important that the equilibrium conditions between the internal and external forces have to be satisfied. Thus, the equilibrium equation for continuum body $\boldsymbol{\Omega}$ with a weak or strong discontinuous boundaryΓ_d, as shown in Figure 20, can be written as

$$\nabla.\mathrm{P} + \mathrm{b} = 0 \tag{6}$$

Where $\boldsymbol{\nabla}$ is the gradient operator, **X** is the Lagrangian coordinate, **b** is body force, and $\boldsymbol{P}$ is the first Piola-Kirchhoff stress tensor (Khoei, 2014). The essential and natural boundary conditions are defined as follows; the displacement boundary condition as $u =$ ~u on Γ_u where ~u is the prescribed displacement on the boundary Γ_u, and the traction boundary condition as $\sigma.n_\Gamma = \_\boldsymbol{t}$ on Γ_t, where $\_\boldsymbol{t}$ is the prescribed traction applied on the boundary Γ_t and n_Γ is the unit outward normal vector to the external boundary Γ. Moreover, the internal boundary condition is defined as $\sigma.n_{\Gamma_d} =\_\ \boldsymbol{t_d}$ on the discontinuity Γ_d, in which $n_{\Gamma_d}$is the unit normal vector to the discontinuity Γ_d. While in a domain wit the strong discontinuity, such as crack interfaces, the traction free condition is assumed as $\sigma.n_{\Gamma_d} = 0$.

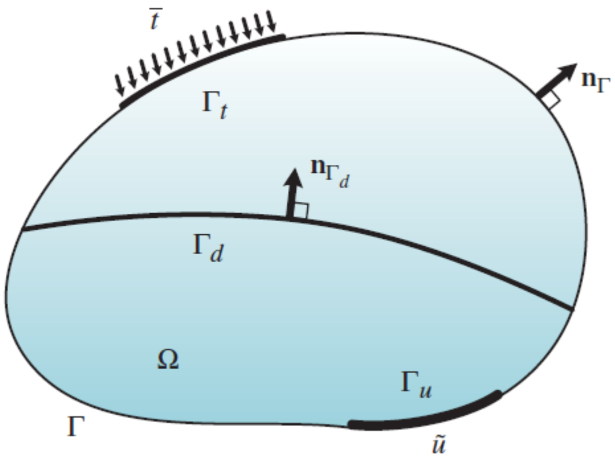

Figure 20: Problem definition of a continuum body Ω with a weak or strong discontinuous boundary Γ_d

The differential equation (6) is written in the reference configuration. In large deformations, the domain of the body in the initial state is denoted by Ω_0 called the initial configuration. In order to describe the deformation of the body, a configuration is used to which the governing equations are referred and is called the reference configuration, Figure 21.

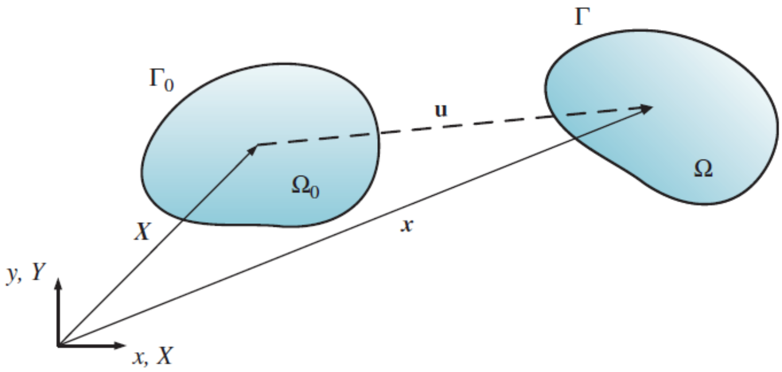

Figure 21: The initial (unreformed) configuration together with the current (deformed) configuration for a continuum body

2.2.2.2 Hardening

The yield and inelastic flow of a metal at relatively low temperatures, where loading is relatively monotonic and creep effects are not important, can typically be described with the classical metal plasticity models. These models use standard Mises or Hill

yield surfaces with associated plastic flow. Perfect plasticity and isotropic hardening definitions are both available in the classical metal plasticity models. Common applications include crash analyses, metal forming, large deformation, and general collapse studies; the models are simple and adequate for such cases.
Most materials of engineering interest initially respond elastically. Elastic behavior means that the deformation is recoverable: when the load is removed, the specimen returns to its original shape. If the load exceeds some limit (the "yield load"), the deformation is no longer fully recoverable. Some part of the deformation will remain when the load is removed, as, for example, when a paperclip is bent too much or when a billet of metal is rolled or forged in a manufacturing process. Plasticity theories model the material's mechanical response, as it undergoes such no recoverable deformation in a ductile fashion. The theories have been developed most intensively for metals, but they are also applied to soils, plastic, rock, ice, crushable foam, and so on. These materials behave in very different ways. For example, large values of pure hydrostatic pressure cause very little inelastic deformation in metals, but quite small hydrostatic pressure values may cause a significant, no recoverable volume change in a soil sample. Nonetheless, the fundamental concepts of plasticity theories are sufficiently general that models based on these concepts have been developed successfully for a wide range of materials.
Most of the plasticity models in finite element solver software's are "incremental" theories in which the mechanical strain rate is decomposed into an elastic part and a plastic (inelastic) part. Incremental plasticity models are usually formulated in terms of

- A yield surface, which generalizes the concept of "yield load" into a test function that can be used to determine if the material responds purely elastically at a particular state of stress, temperature, etc.;
- A flow rule, which defines the inelastic deformation that occurs if the material point is no longer responding purely elastically; and

- Evolution laws that define the hardening—the way in which the yield and/or flow definitions change as inelastic deformation occurs

In finite element solver, software a perfectly plastic material can be defined, or work hardening can be specified.

Isotropic, kinematic, and Johnson-cook are common hardening used in finite element solver software. Isotropic hardening means that the yield surface changes size uniformly in all directions such that the yield stress increases (or decreases) in all stress directions as plastic straining occurs. Abaqus provides an isotropic hardening model, which is useful for cases involving gross plastic straining or in cases where the straining at each point is essentially in the same direction in strain space throughout the analysis. If isotropic hardening is defined, the yield stress,, can be given as a tabular function of plastic strain and, if required, of temperature and/or other predefined field variables. The yield stress at a given state is simply interpolated from this table of data, and it remains constant for plastic strains exceeding the last value given as tabular data. Johnson-Cook hardening is a particular type of isotropic hardening where the yield stress is given as an analytical function of equivalent plastic strain, strain rate, and temperature. This hardening law is suited for modeling high-rate deformation of many materials including most metals. Also the Johnson-Cook hardening used for dynamic analysis.

Two kinematic hardening models are provided in finite element solver software to model the cyclic loading of metals. The linear kinematic model approximates the hardening behavior with a constant rate of hardening. The more general nonlinear isotropic/kinematic model will give better predictions but requires more detailed calibration.

In this, study as described above and run analysis with different hardening the isotropic hardening give more accurate result than kinematic hardening.

2.3 Material Characterization

For the thesis, the base of the study is on the polymer foams, the VeroWhite plastic is chosen. VeroWhite is a popular polymer which is using in different kind of industry and medicine. A unique combination of low Water Absorption value (ASTM D570-98 24Hr) and heat deflection temperature (ASTM D-648) enables VeroWhite models to preserve their dimensions in the kind of environmental conditions that models are exposed during transit. VeroWhite also offers excellent flexural strength and flexural modulus along with tensile strength making it ideal for engineering simulation and structural testing. With the superb surface quality and detail visualization of the opaque, rigid VeroWhite material, models look and feel like molded plastic parts. This is valuable whenever plastic simulation is required, such as for toys, automotive products, consumer goods and electronics, medical equipment, piping and more. While VeroWhite is more capable for prototyping industry applications: medical Models, dental Industries, dental Labs, rapid Tooling, consumer products, marketing and sales. With this benefits in our study the VeroWhite material choice.

Material data is very important during AM progress because the AM produce product layer by layer, in fact, AM product has anisotropic behavior. Meanwhile, to define the material data, a test sample product and tensile tested on the model with our partner, Pittsburgh university .The bulk sample of VeroWhite for experimental test printed at six different way. They named as XY, YX, ZX, XZ, YZ, and ZY. The X, Y, and Z all indicate printing direction. X and Y are thin-plane directions, while Z is the printing direction. They are rectangular bars. The first character (e.g. in XY, XZ) means the longitudinal direction of the tensile bar and, of course, the loading direction. The second character here is the width direction of the tensile bar. So all the tensile bars with X and Y as initial are printed in plane, which are usually ductile. However, the tensile bars with Z as the initial are printed normal to the plane, which are brittle. Since the properties are not uniform, Using the average modulus and yield stresses to do the simulation for other structures.

The first attempt for homogenization of cellular structure used original model tensile test results for determining cellular structure material model properties such as true stress, true plastic strain, and Young’s modules. In order to analyze the cellular structure compression force on displacement boundary conditions is applied. In such a case, to improve the homogenization of cellular structure results, we need to obtain compression stress-strain curve from the original material. The original model tensile test was simulated at commercial finite element software, and the FEA result was compared with experimental tensile results. After reaching a delicate approximation between the finite element simulate and experimental result for tensile, we simulated compression test and defined the true plastic strain, true stress, and Young’s modulus. This result gives us notable improvement for those errors during first period analysis.

2.3.1 Finite element modeling of original bulk sample

Since AM the material layer by layer, for simulating the bulk model, we assumed models such as composite material. For substantiation of our theory, the tensile test was simulated and compared with experimental results. With good estimations of material mechanical property values, the compression analysis was done. The finite element modeling test sample geometry is 2mm wide and has a 9 mm length, and extrudes 18mm. The shape of the tensile test specimen is shown in Figure 22.

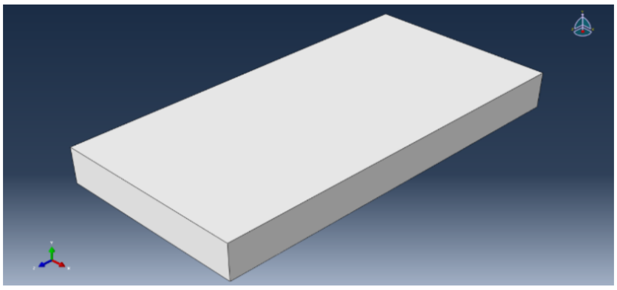

Figure 22: Tensile Test Specimen

Elements SC8R are employed and are described as an 8-node quadrilateral in-plane general-purpose continuum shell. This mesh contains 40,500 elements. The mesh is a reduced integration with an hourglass control and finite membrane strains. The material properties are converted into true stress and true plastic strain from the nominal stresses and nominal strains, shown in equation (6), in order to satisfy the material input requirement's.

$$\sigma_{tru} = \sigma_{nom}(1 + \varepsilon_{nom}) \tag{7}$$

$$\varepsilon_{tru} = \ln(1 + \varepsilon_{nom})$$

$$\varepsilon_{pl} = \varepsilon_{tru} - \frac{\sigma_{tru}}{E} \tag{8}$$

The model was displaced with an initial value of 1.15mm in the axial direction, and the other end has a fixed condition. A representation on the ply-stack up for 11 ply model in the [0/90] orientation is shown in Figure 23. The mesh is shown in Figure 24.

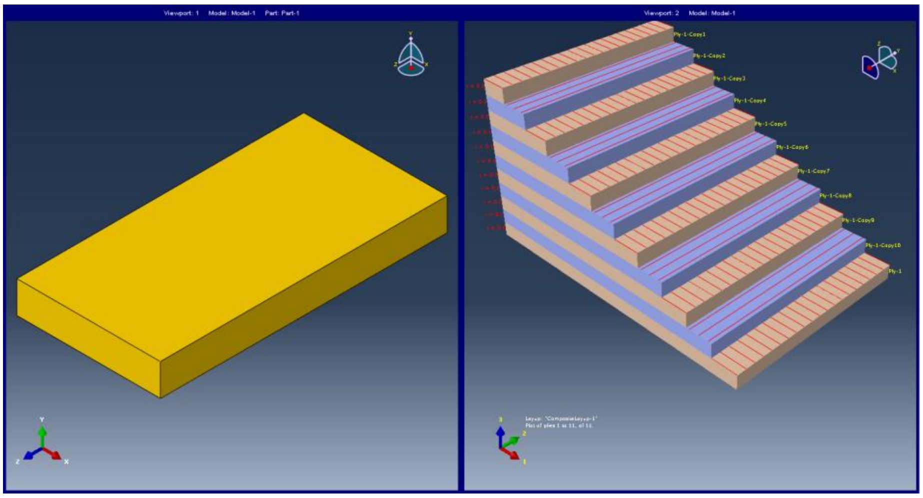

Figure 23: Ply Stack Up

The composite layer material properties are shown in Table 2.

Table 2: Composite Layer Properties

E1	E2	Nu12	G12	G13	G23
1698.2	1721.63	0.39	389.503	389.503	389.503

The data for composite layer material properties given in the table above resulted from the described experimental method.

The finite element modeling software assumes prefect bonding between layers, which VeroWhite Additive manufactured parts do not have. Bonding strength between filament in the 2-direction is assumed to be the same in the 2-Z direction. In order words $E_{22}=E_{23}=E_{13}$, $G_{12}=G_{22}=G_{13}$, $\vartheta_{12} = \vartheta_{23} = \vartheta_{13}$.

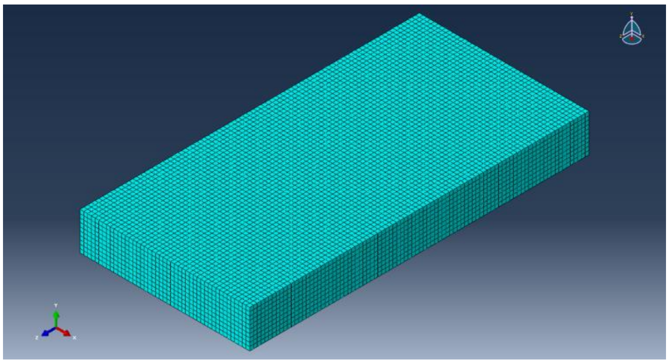

Figure 24: Composite Tensile Test Mesh

2.3.2 Tensile test simulation

The axial direction for tensile test is defined on the Z direction. The left side applies1.15mm displacement while the other side is fixed. The static non-linear analysis was running due to define load-displacement curve.

The resulting load-displacement from the composite FEA tensile model is converted to stress-strain shown in Figure 25. Figure 26 compares the FE analysis with the experimental tensile test. The result from the FEA model gives a good estimate from experimental tensile test. As one can see, other than the shown four percent error, the two results match rather well.

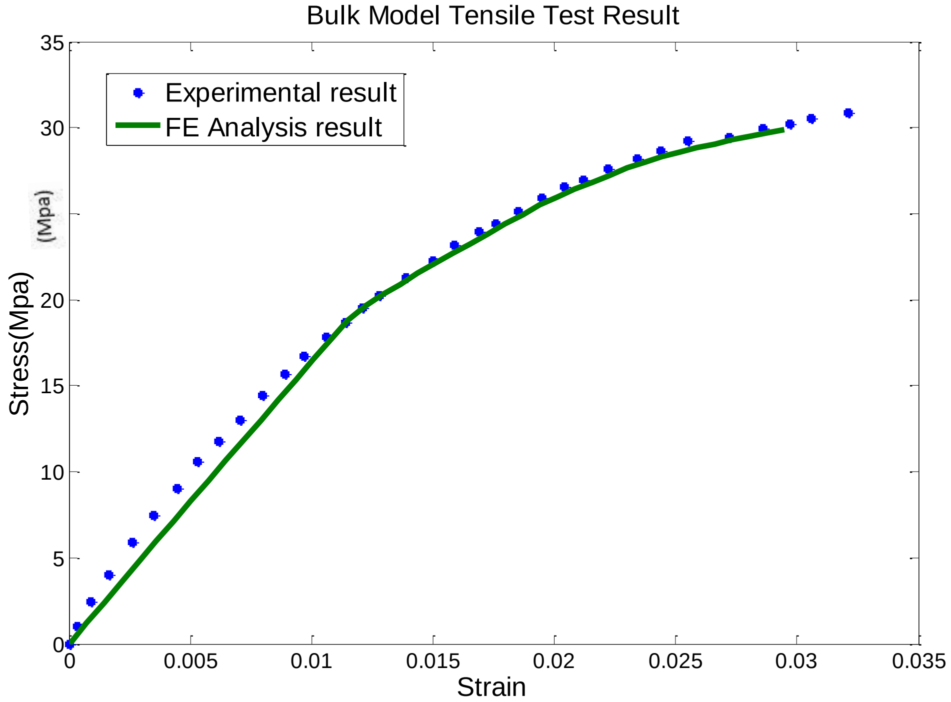

Figure 25: The FEA vs. experimental tensile test

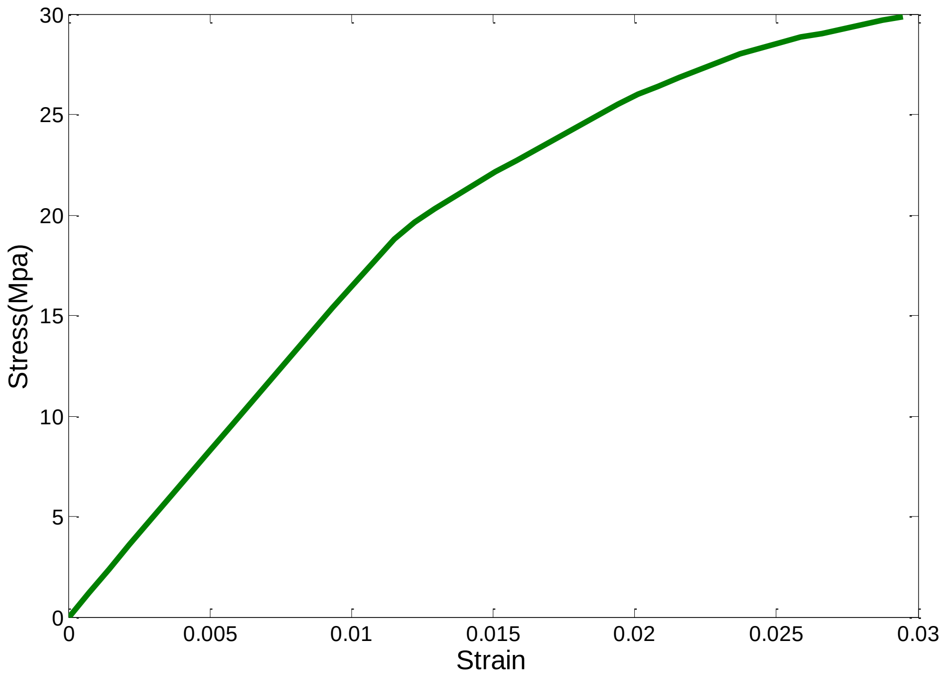

Figure 26: FEA Tensile test

2.3.3 Compression test simulation

The same geometry and mesh above were modeled in finite element modeling software as compression. The true plastic strain and true stress are the same as the tensile model. The model is displaced by initial value of -1.15mm in the axial direction, and the other end has a fixed condition.

The stress-strain curve results from the load-displacement from the FEA modeled. The Figure 27 shows the compression stress on the displacement direction.

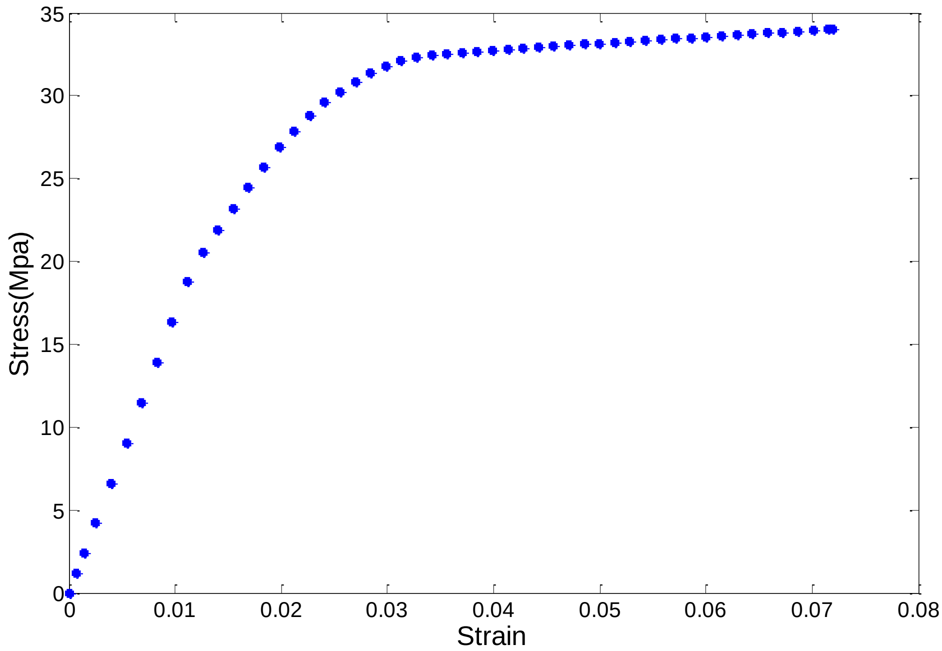

Figure 27: FEA Compression test

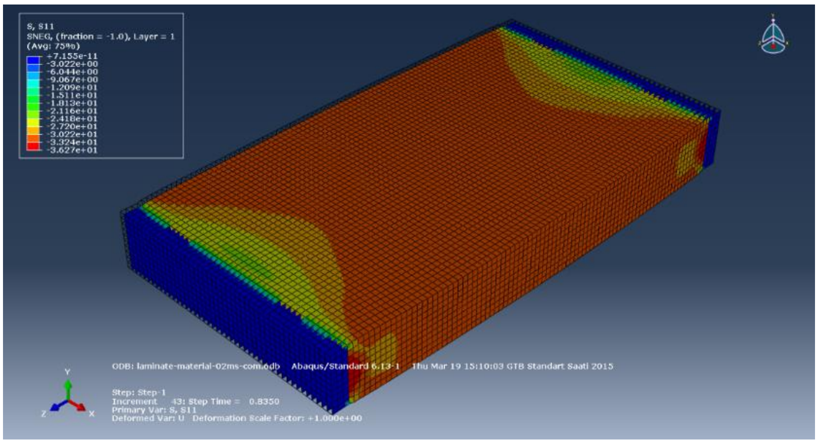

Figure 28: Composite, Compression analysis (11 Ply [0/90]).

The stress-strain curve that resulted from the compression test was used to bring about the new true plastic strain and true stress, which were then used to improve the cellular structure analysis.

2.4 Static Nonlinear Finite Element Modeling Isotropic Hardening

During the analysis the compression was done one the cellular structures. For the boundary condition the 1.15mmdisplacement was applied. The displacement is expected to produce plastic deformation. The other side of the models was fixed. After the analysis was finished during the post process the load-displacement curve was obtained. In the excel post processing result, the load-displacement curve, was utilized to obtain stress-strain curve. The Figures 29(a), 30(a), 31(a), 32(a), and 33(a) show the stress-strain curves of the foams with relative density of 0.4, 0.35, 0.3, 0.25, and 0.2 respectively. The Figures 29(b), 30(b), 31(b), 32(b), and 33(b) shown the stress distribution of foams with relative density of 0.4, 0.35, 0.3, 0.25, and 0.2, respectively. The Comparison of stress-strain curve for foams with relative density of 0.4, 0.35, 0.3, 0.25, and 0.2 shown in the Figure 34.

a)

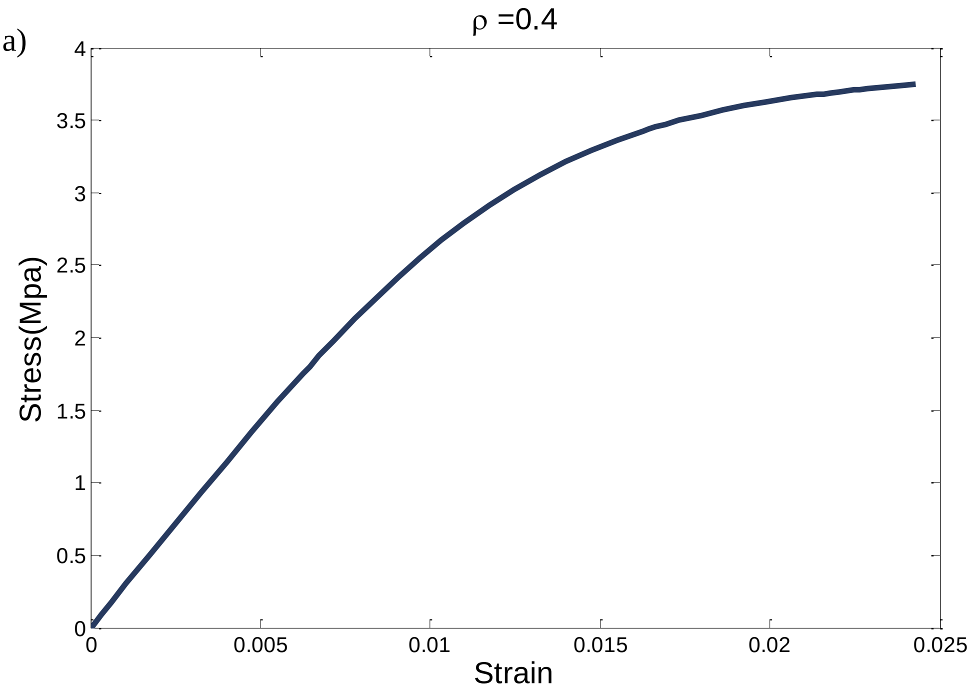

b)

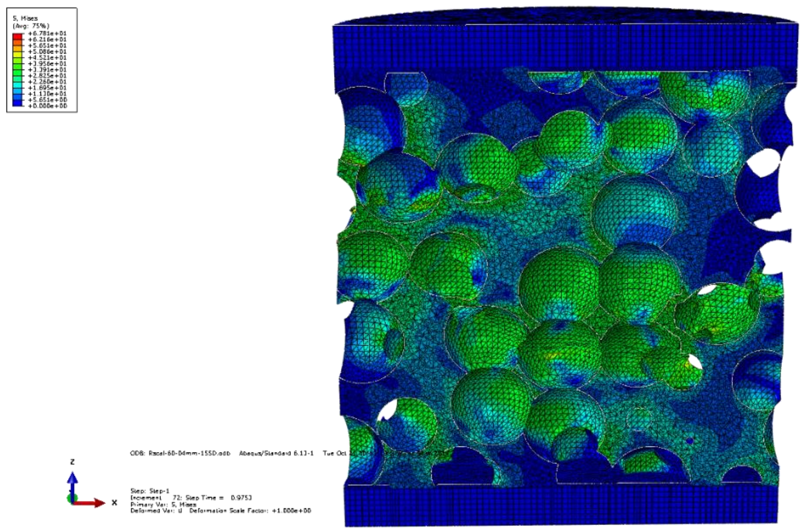

Figure 29: Stress-strain curve (a) and isotropic compression test model (b) for ρ= **0.4**

a)

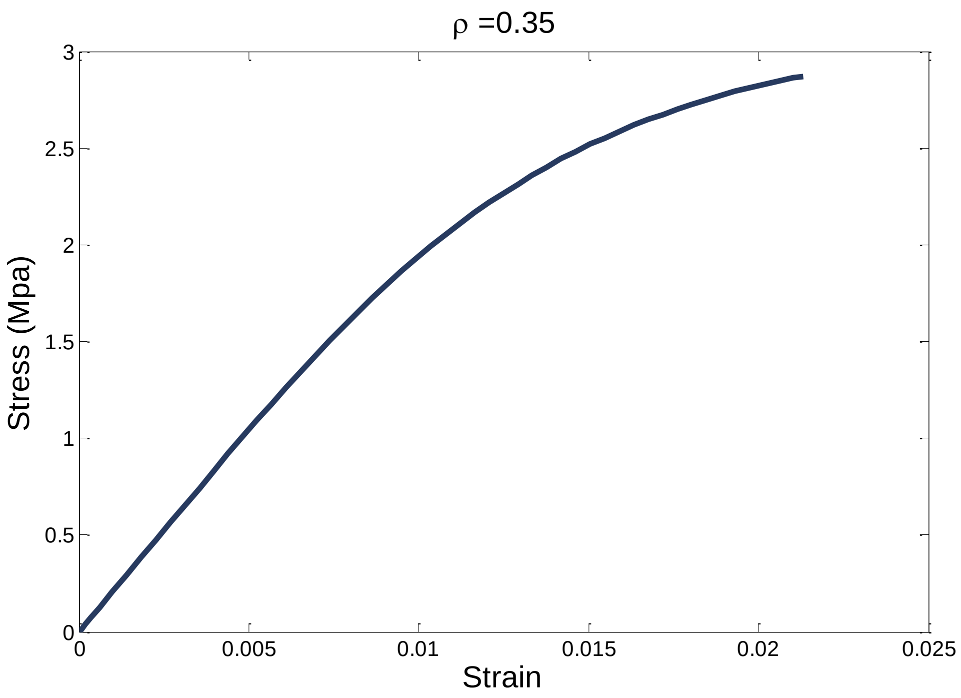

b)

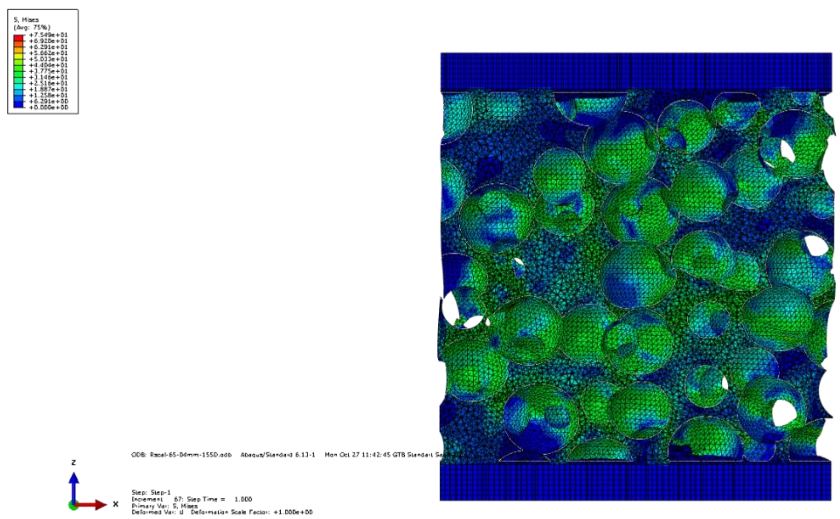

Figure 30: Stress-strain curve(a) and isotropic compression test model (b) for ρ= $\mathbf{0.35}$

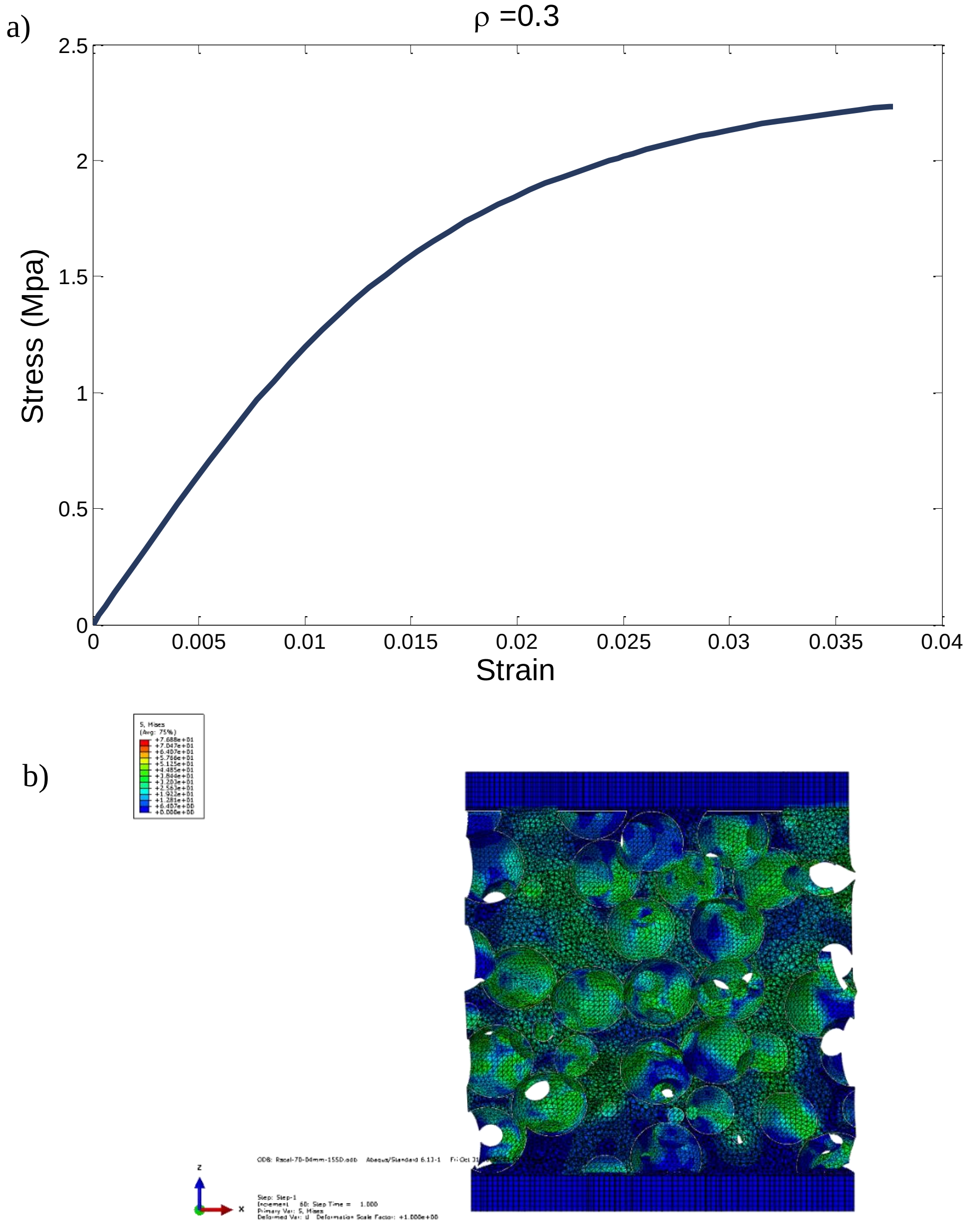

Figure 31: Stress-strain curve (a) and isotropic compression test model (b) for $\rho = \mathbf{0.3}$

a)

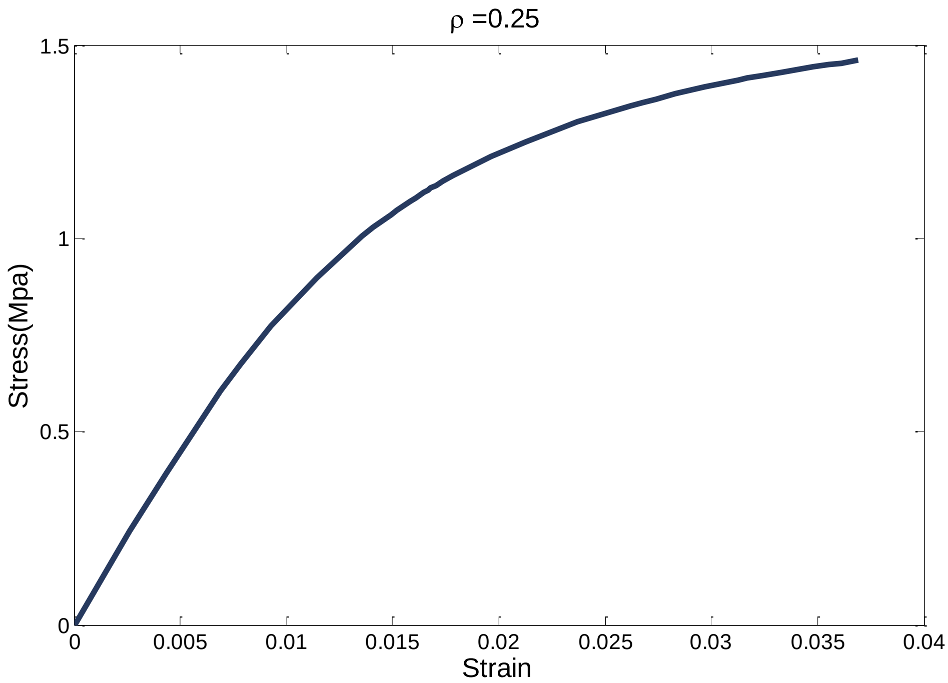

b)

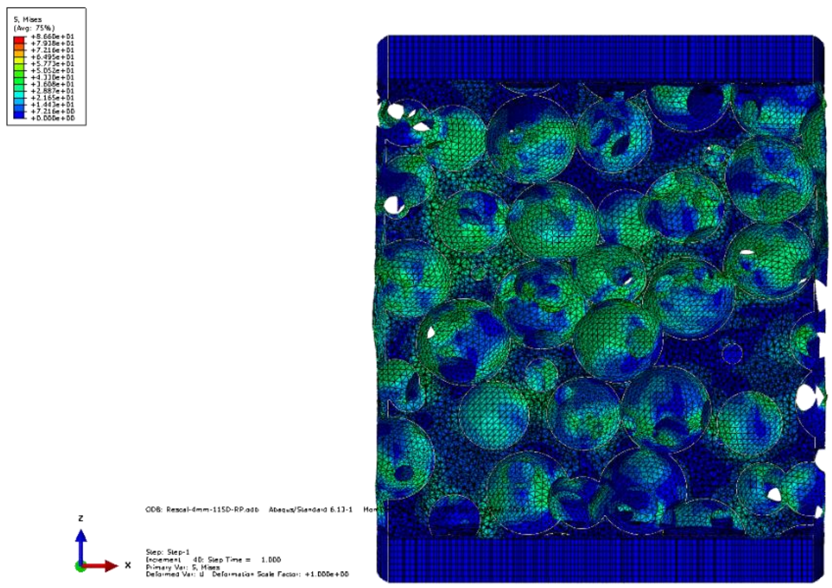

Figure 32: Stress-strain curve (a) and isotropic compression test model (b) for ρ= $\mathbf{0.25}$

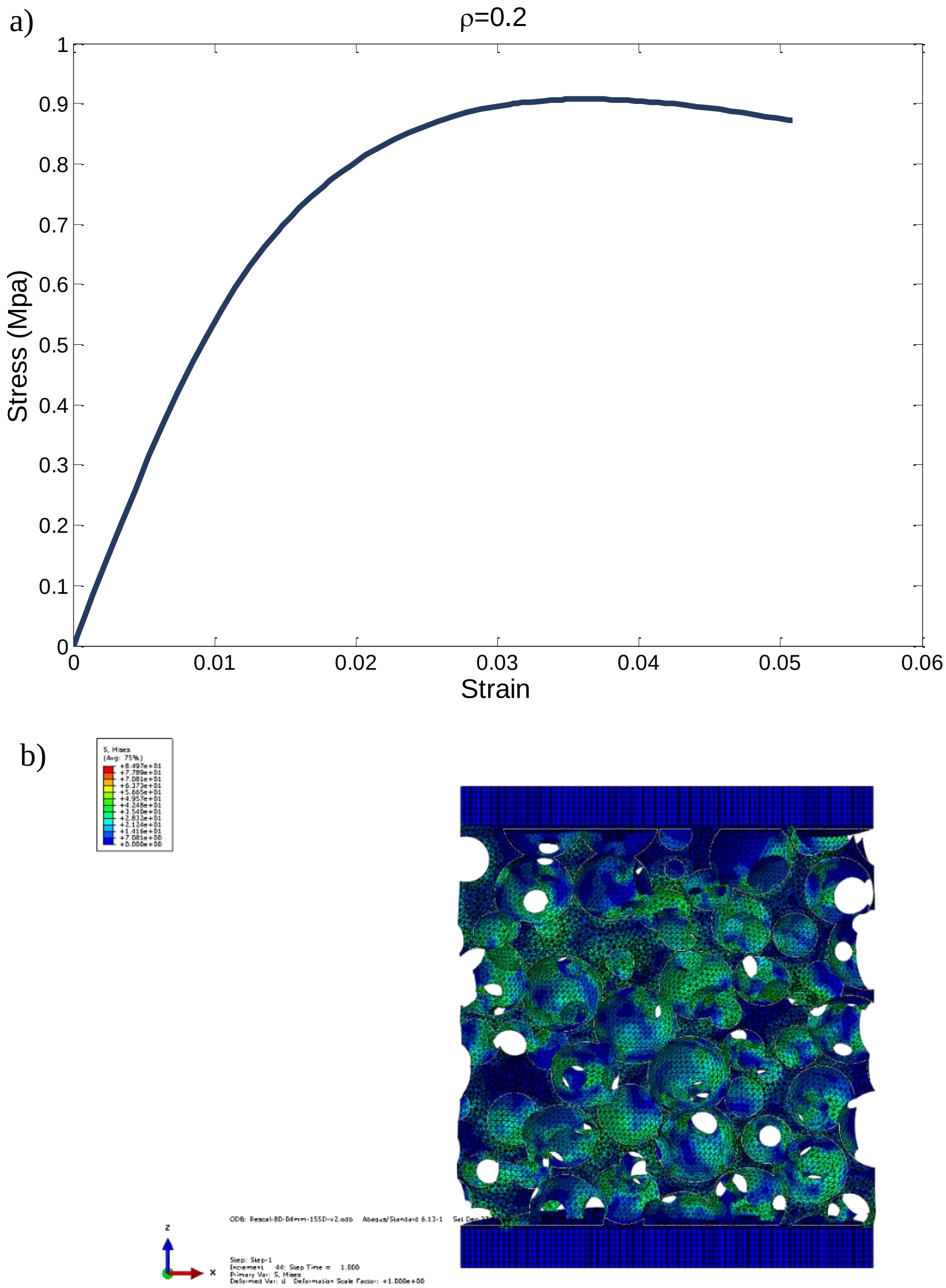

Figure 33: Stress-strain curve (a) and isotropic compression test model (b) for ρ= $\mathbf{0.2}$

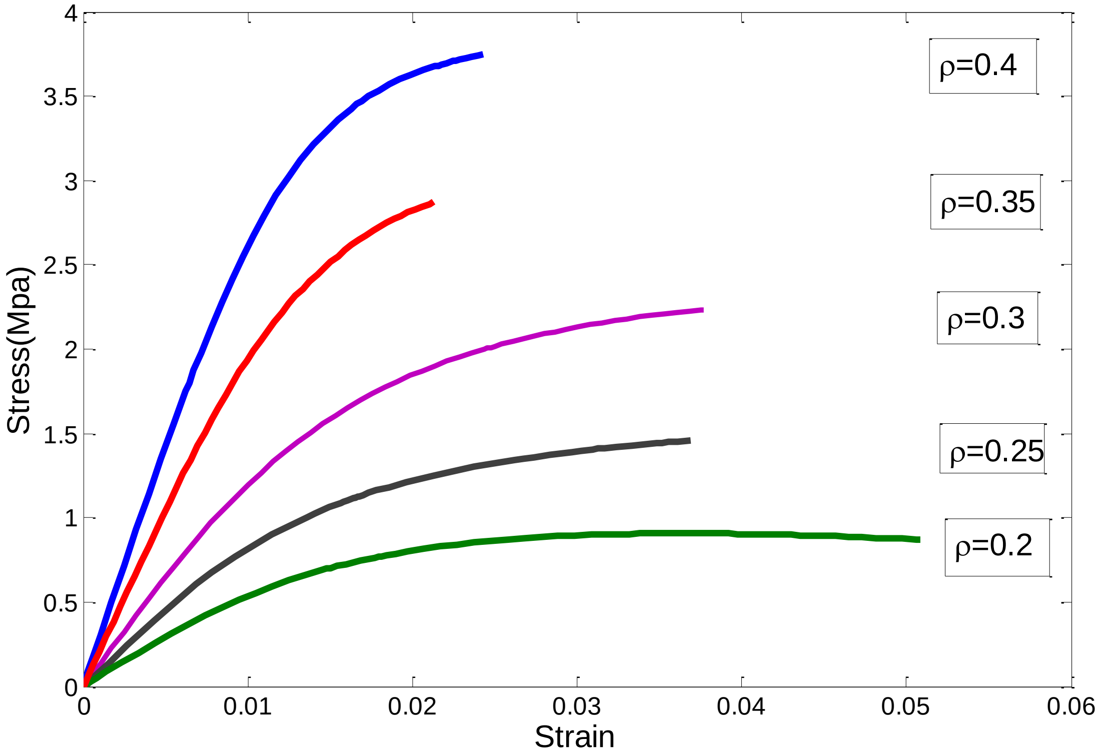

Figure 34: Based on relative density comparison of cellular models

2.4.1 Finite element modeling, damping facture

During the static analysis for the models with high relative density, there observed more energy absorption than the low relative density models, such a models $\rho/\rho^* = 0.4$.

To obtain the value of energy absorption the automatic stabilization was used. Automatic stabilization utilized for nonlinear unstable problem. However, if the instability is localized, there will be a local transfer of strain energy from one part of the model to neighboring parts. To solve this type of problem in literature suggested either dynamically or with the aid of damping. In addition, the volume-proportional damping the quasi-static step may result reasonable accuracy. Viscos forces of the form are being add to the global equilibrium equations

$$\mathrm{F_v} = \mathrm{cMv} \tag{9}$$

$$\mathrm{P} - \mathrm{I} - \mathrm{F_v} = 0 \tag{10}$$

where, M is an artificial mass matrix calculated with unity density, c is damping factor, $v = \Delta u/\Delta t$ is the vector of nodal velocities, and Δt is the increment of time.

2.5 Experimental Testing of Cellular Structure Models

For compression testing on cellular structure, following ASTM standard utilized. The ASTM D-695 ((ASTM), 2010)standard test method is for compressive properties of rigid plastics. This test (ASTM D-695) method covers the determination of the mechanical properties of unreinforced and reinforced rigid plastics, including high modulus composites or cellular structures, when loaded in compression at relatively low uniform rates of straining or loading.

Figure 35: MTS 880 system for compression test.

The test machine is an MTS 880 system for compression testing. The MTS 880 is a servo hydraulic universal testing machine. The maximum force capacity is 10 ton in compression/tension. The MTS 880, the tensile testing, fatigue, compression, bending, simple shear, and creep is done.

From the MTS 880 result, the stress- strain curve obtained. They are shown in the Figures 36(a), 37(a), 38(a), 39(a), and 40(a) for the foams with relative density of 0.4, 0.35, 0.3, 0.25, and 0.2, respectively. The printed foams with relative density of 0.4, 0.35, 0.3, 0.25, and 0.2, shown in Figures 36(b), 37(b), 38(b), 39(b), and 40(b), respectively.

The Figure 40 show the comparison of foams with relative density of 0.4, 0.35, 0.3, 0.25, and 0.2, stress-strain curve.

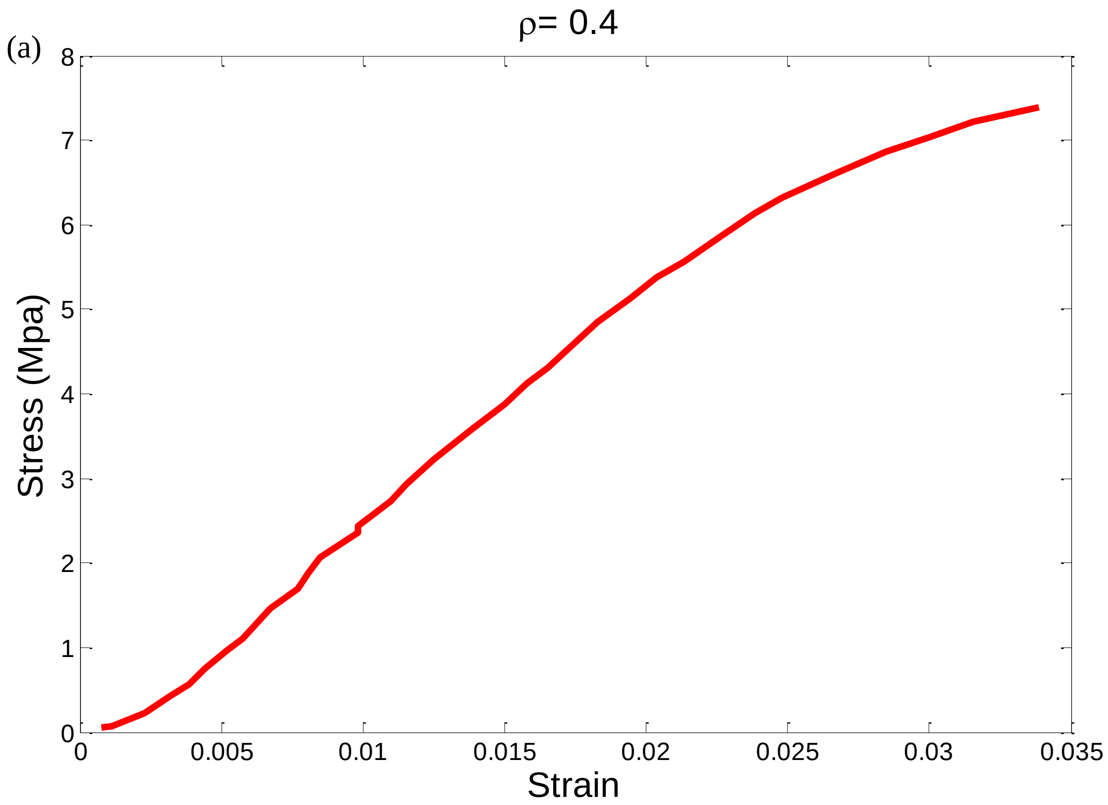

Figure 36: Stress-strain curve (a) and the AM manufactured cellular structure (b) for $\boldsymbol{\rho = 0.4}$

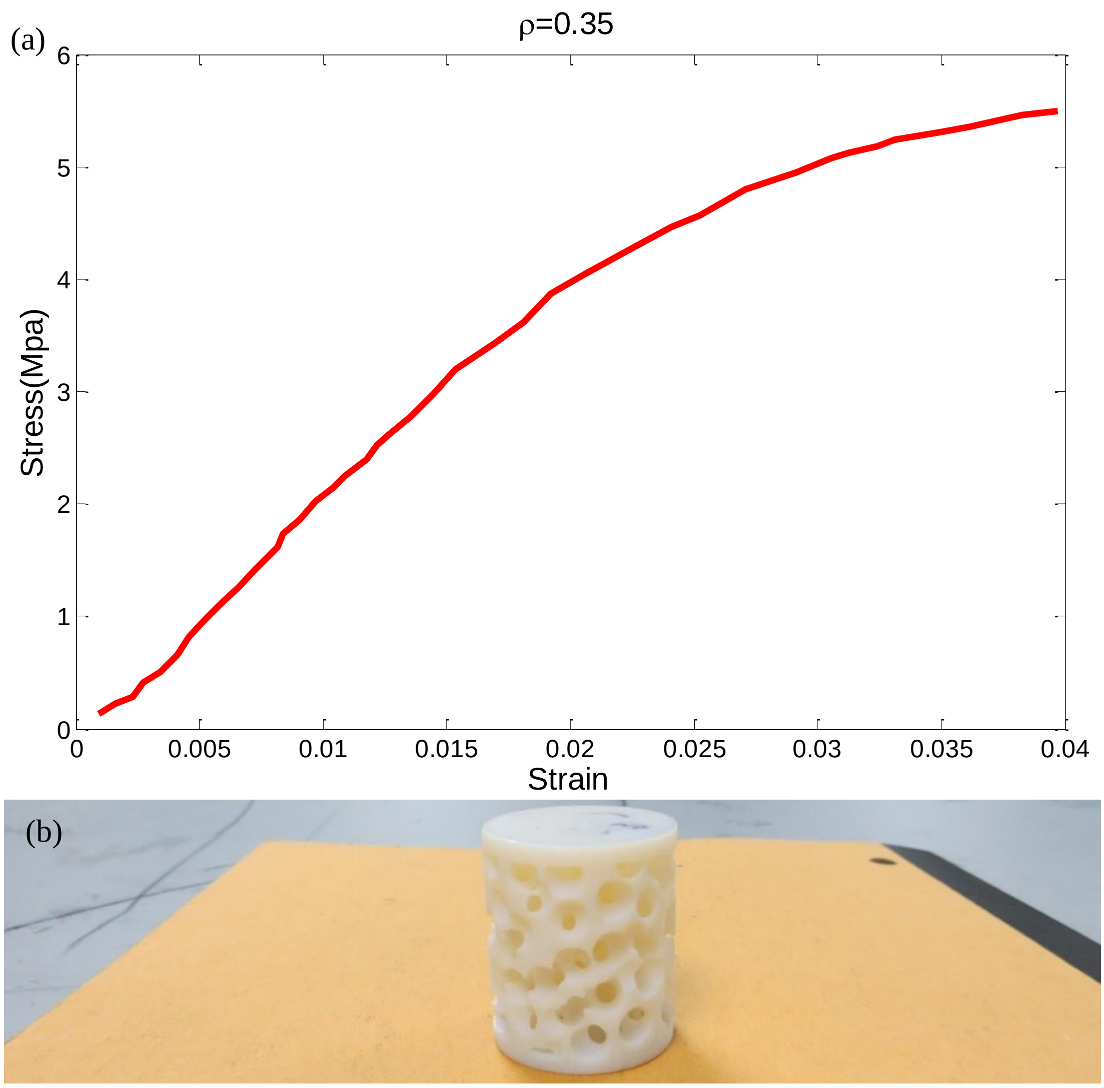

Figure 37: Stress-strain curve (a) and the AM manufactured cellular structure (b) for $\boldsymbol{\rho = 0.35}$

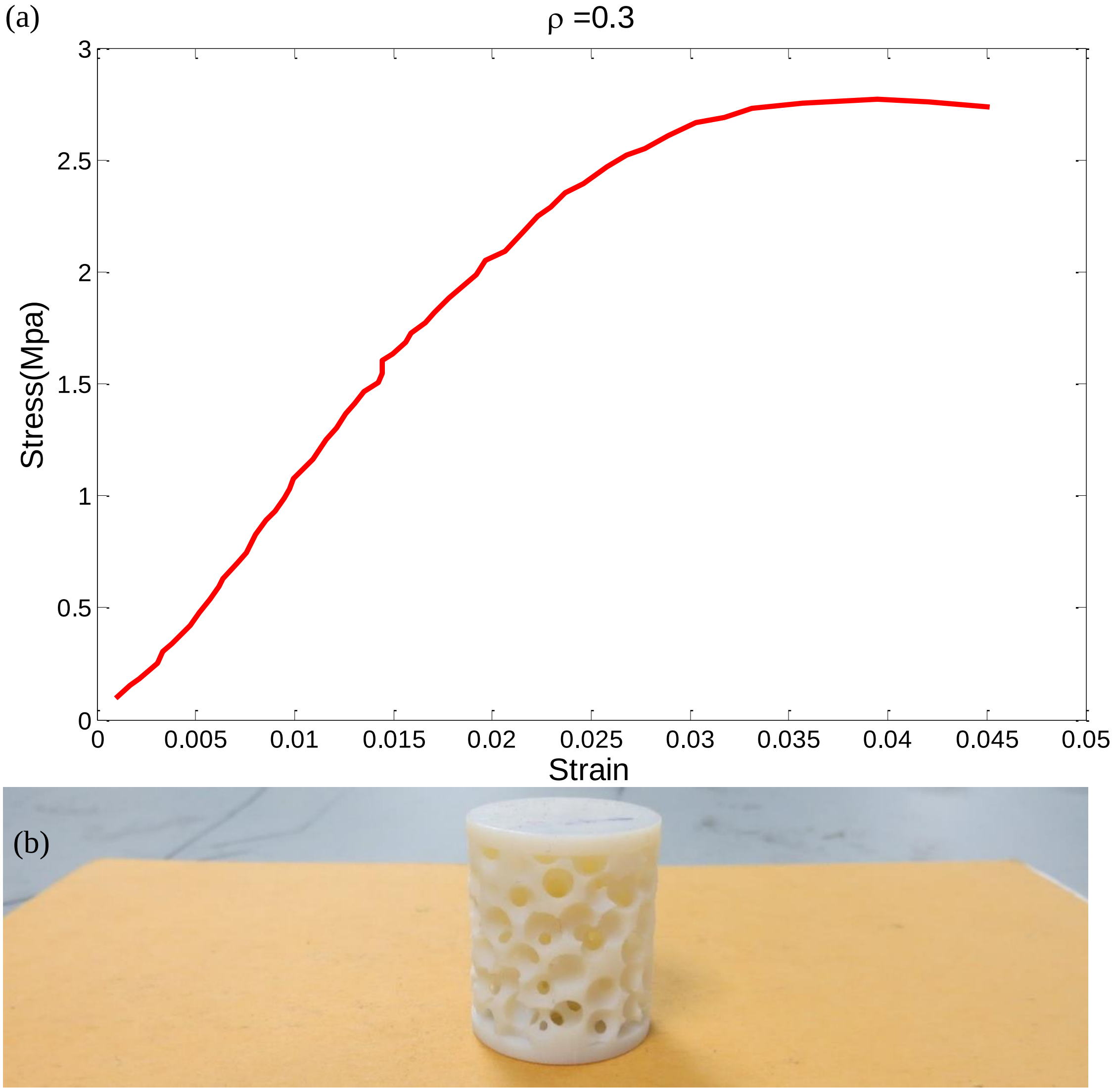

Figure 38: Stress-strain curve (a) and the AM manufactured cellular structure (b) for $\boldsymbol{\rho = 0.3}$

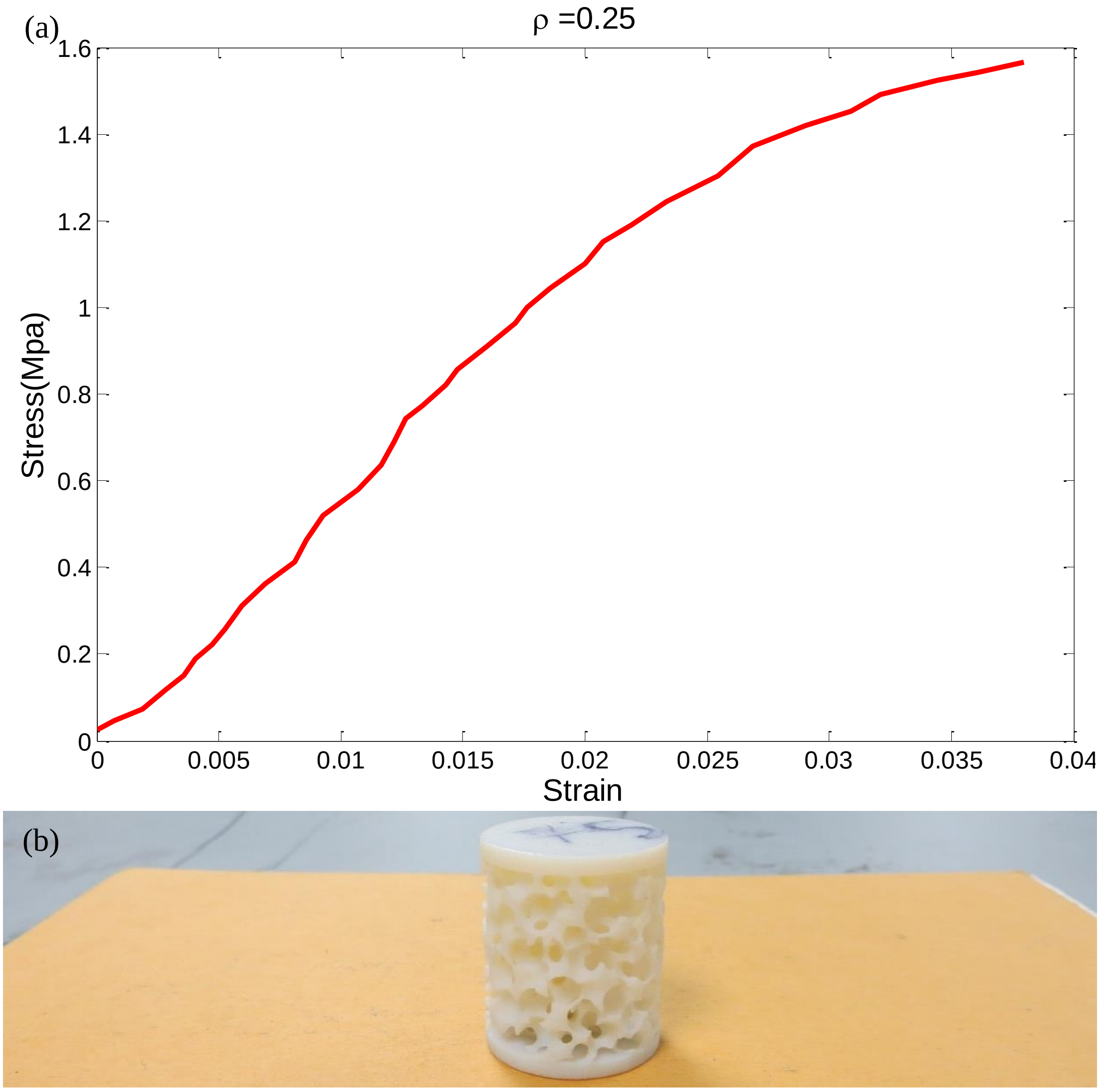

Figure 39: Stress-strain curve (a) and the AM manufactured cellular structure (b) for $\boldsymbol{\rho = 0.25}$

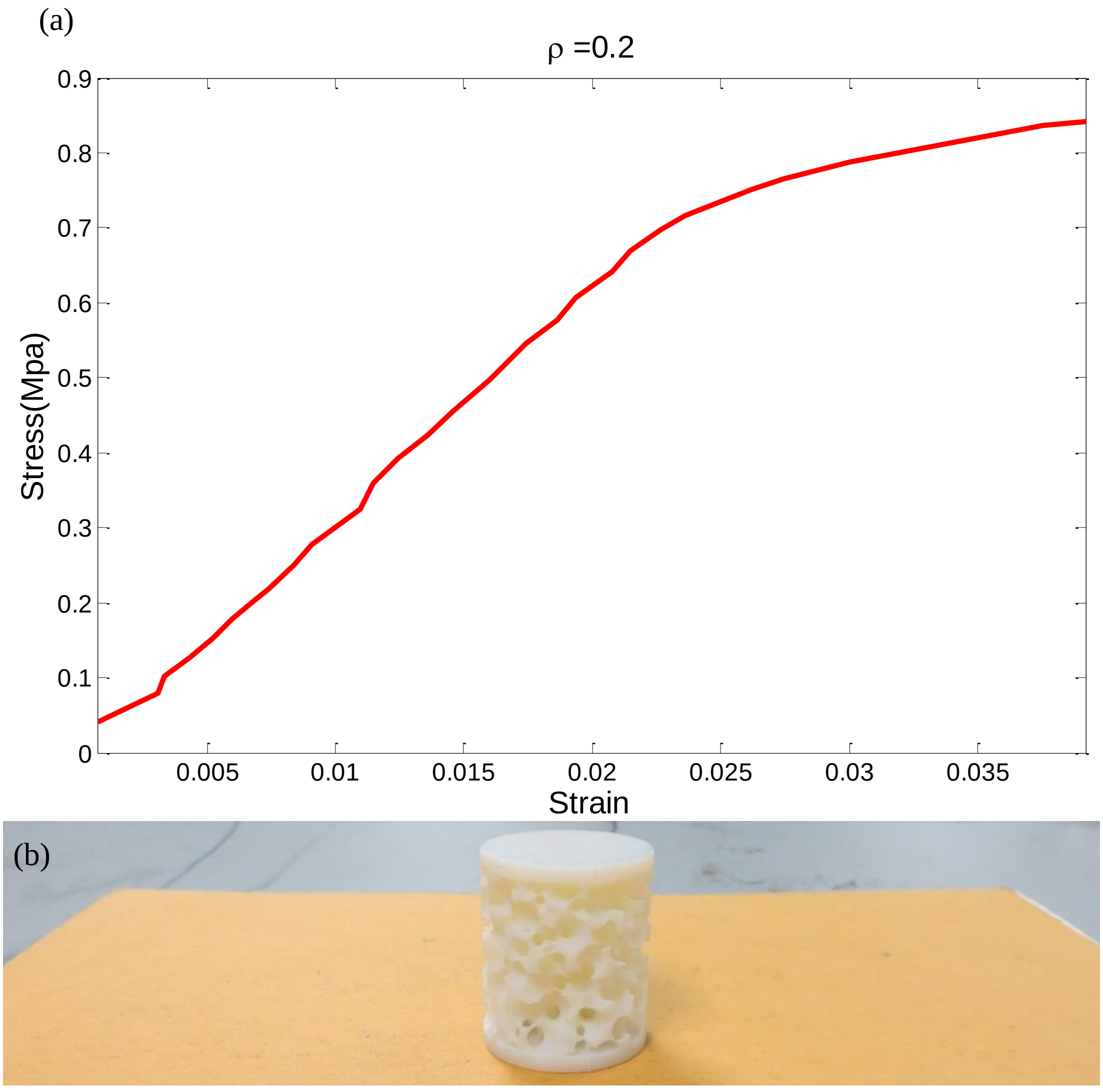

Figure 40: Stress-strain curve (a) and the AM manufactured cellular structure (b) for $\boldsymbol{\rho = 0.2}$

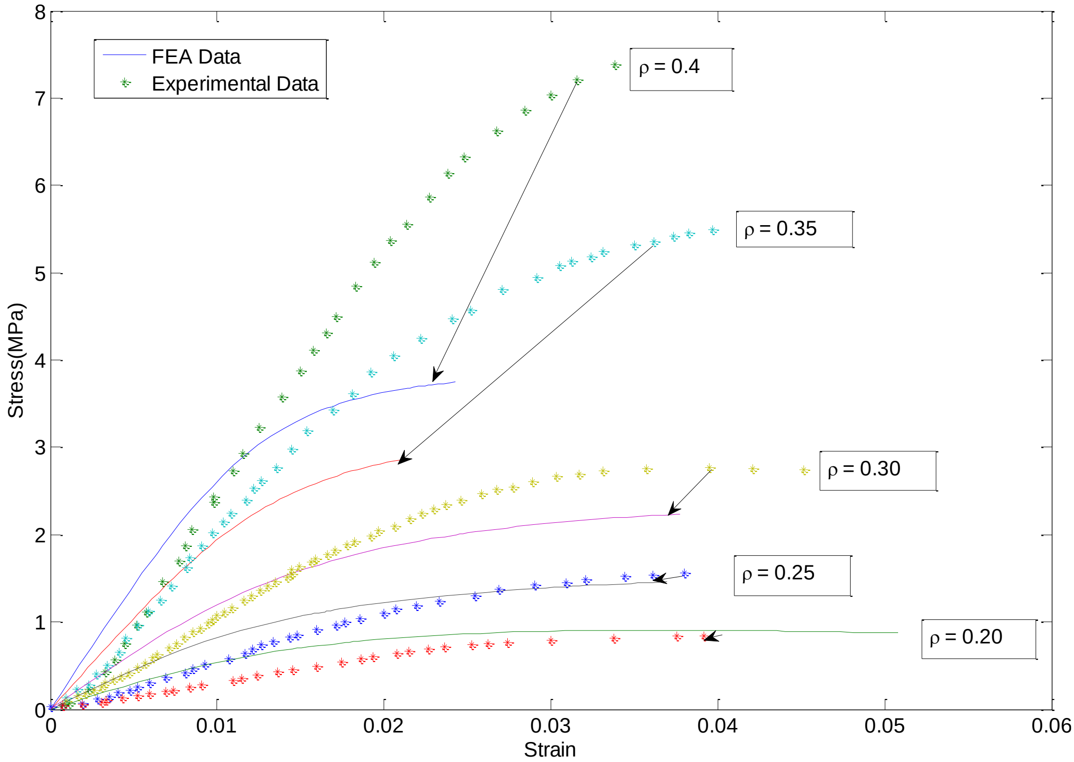

Figure 41: Based on relative density comparison of cellular models

3. HOMOGENIZATION STUDY

During additive manufacturing cellular structure for reduce material are used, and slightly mechanical properties, in case of minimize the overall cost, additive manufacturing cellular structures need computational methodology to optimize the design. In literature (Pu Zhang, et al., 2015) propose three key steps for designing process: homogenization, optimization, and construction (HOC). Homogenization as a first steps, needs to traverse discontinuous solid into a continuous model by representing its microstructure character such as relative density and orientation.

3.1 Gibson-Ashby Model

Two types of cellular material usually are considered, as closed cells which surrounded by edges and join together to form vertices. Second type is open cells. The cellular structure is characterized by relative density, cell size, and cell shape, which density is the accrue way measured with weighting a sample. The Gibson-Ashby model is often used density of foams relative with original material and called it relative density. While looking at this model, the elastic modulus E, and yield stress σ_{pl} of cellular material have power law relationships or scaling law. The scaling law bonded to average density$\rho(x)$.

The formulations of the three regions are:

- Linear elastic region:

$$\begin{gathered}\sigma = \mathrm{E}\varepsilon \\ \text{If } \sigma \leq \sigma_{\mathrm{yield}}\end{gathered} \tag{11}$$

- Plateau region:

$$\sigma = \sigma_{\mathrm{yield}} \tag{12}$$

$$\text{if } \varepsilon_{\text{yield}} \le \varepsilon \le \varepsilon_{\text{D}}(1 - \text{D}^{-\frac{1}{\text{m}}})$$

- Densification region:

$$\sigma = \sigma_{yield}\frac{1}{D}\left(\frac{\varepsilon_D}{\varepsilon_D - \varepsilon}\right)^m$$

$$\text{if } \varepsilon > \varepsilon_{\text{D}}(1 - \text{D}^{-\frac{1}{\text{m}}}) \tag{13}$$

3.2 Homogenization

Conventional cellular structure mechanical properties depend on the material component, the relative density, and the detailed cell structure (Pu Zhang, et al., 2015). Following the Gibson-Ashby models (F.Ashby, et al., 2000) the elastic modulus E and yield stress $\sigma_{pl}$of cellular structures have polynomial law relationships, or scaling law, with respect to the relative density ρ(x).

According to the literature (Pu Zhang, et al., 2015), for the anisotropic constitutive law $\sigma = \boldsymbol{C}\varepsilon$ is used, where σ, **C**, and ε are the stress, elastic matrix, and the strain, respectively. For a plan stress problem we have, Equation (3).

The polynomial function used for fitting the scaling law can be written as relative density function:

$$\boldsymbol{C}(\rho) = \boldsymbol{C}_0 + \boldsymbol{C}_1\rho + \boldsymbol{C}_2\rho^2 + \cdots$$

where, $\boldsymbol{C}_i(i = 0, 1, 2, \dots)$ are constant symmetric matrices to be determined.

For our study, these constants were determined for static nonlinear finite element model, quasi-static nonlinear finite element model with damping factor, and experimental compression result.

3.3 Homogenization with Experimental Data

Equation (4) is for the generalized anisotropic case, which can lend simplified for orthotropic or isotropic cases. In our study, spherical cells structures, which is three-dimensional isotropic material. In fact, there are only two independent material constants in the material elastic matrix **C**, as $\boldsymbol{C}_{11}$ and $\boldsymbol{C}_{33}$.other constant in the elastic matrix can be eliminate from the relationships $\boldsymbol{C}_{22} = \boldsymbol{C}_{11}, \boldsymbol{C}_{12} = \boldsymbol{C}_{11} - 2\boldsymbol{C}_{33}, and\ \boldsymbol{C}_{13} = \boldsymbol{C}_{23} = 0$. The experimental test is done to define the relative Young's modulus and relative yield strength, which are shown on Figure 42 for relative Young's modulus and Figure 43 for relative yield stress. The scaling law for relative Young's modulus is:

$$2.461\rho^2 - 0.6898\rho + 0.05574 = E/E^* \qquad (14)$$

And the scaling law for relative yield strength is:

$$2.917\rho^2 - 0.7369\rho + 0.05598 = \sigma/\sigma^* \qquad (15)$$

Table 3: Homogenization table FEA result

	ρ	σ (Mpa)	E (Mpa)	E/E*	σ/σ*
FEA Result	0.2	**0.80**	**42.78**	**0.03**	**0.03**
	0.25	**1.18**	**71.92**	**0.04**	**0.05**
	0.3	**1.70**	**119.65**	**0.07**	**0.07**
	0.35	**2.52**	**199.49**	**0.12**	**0.11**
	0.4	**3.21**	**271.17**	**0.16**	**0.14**

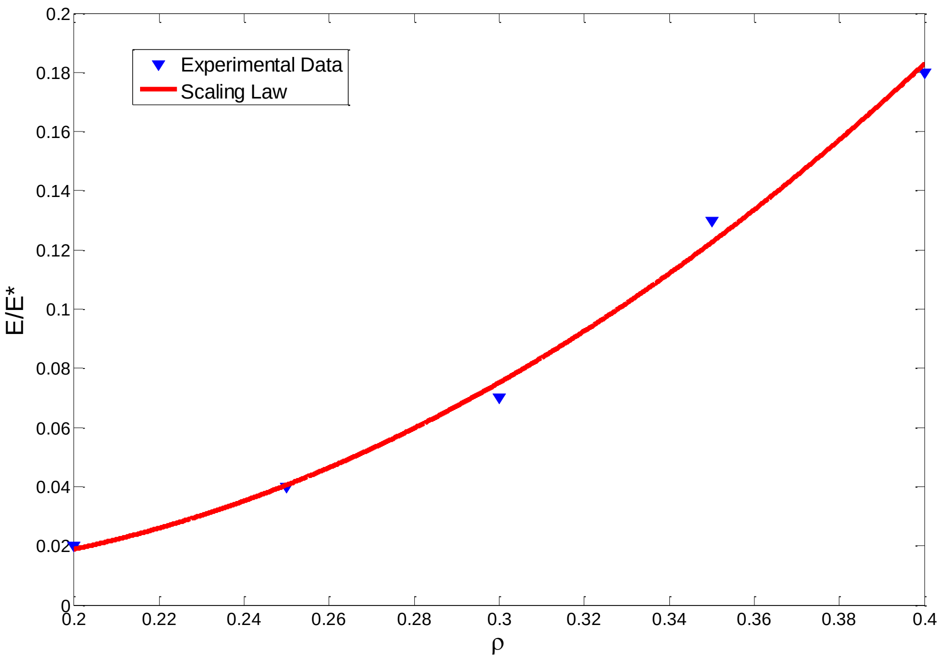

Figure 42: Experimental test result for relative Young's modulus.

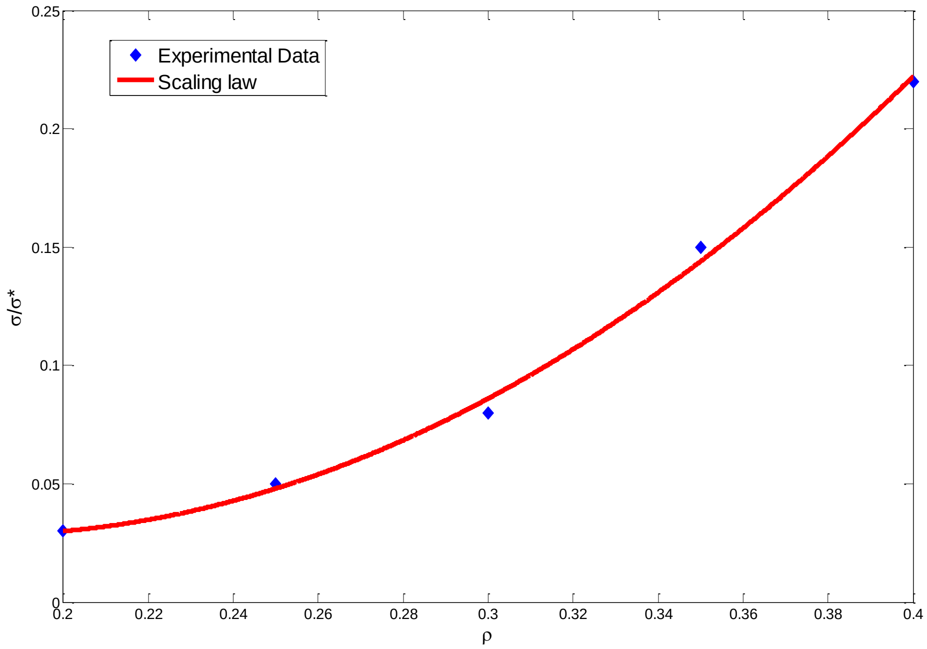

Figure 43: Experimental test result for relative Yield strength

3.4 Homogenization with Finite Element Modeling Data

Same as the experimental compression test, the FEA simulated ran on the finite element commercial software. Here, the result fit the scaling law for this spherical cells structure. The relative Young's modulus, Figure 44, and the relative yield strength, Figure 45, are considered as a function of density. The scaling law for Young's modulus is:

$$1.916\rho^2 - 0.4809\rho + 0.04291 = E/E^* \tag{16}$$

And the scaling law for relative yield strength is:

$$0.9446\rho^2 - 0.00841\rho + 0.007367 = \sigma/\sigma^* \tag{17}$$

Table 4: Homogenization table Experimental result

	ρ	σ (Mpa)	E (Mpa)	E/E*	σ/σ*
Experimental Result	0.2	**0.75**	**32.17**	**0.02**	**0.03**
	0.25	**1.15**	**60.48**	**0.04**	**0.05**
	0.3	**1.92**	**112.52**	**0.07**	**0.08**
	0.35	**3.43**	**220.15**	**0.13**	**0.15**
	0.4	**5.12**	**295.89**	**0.18**	**0.22**

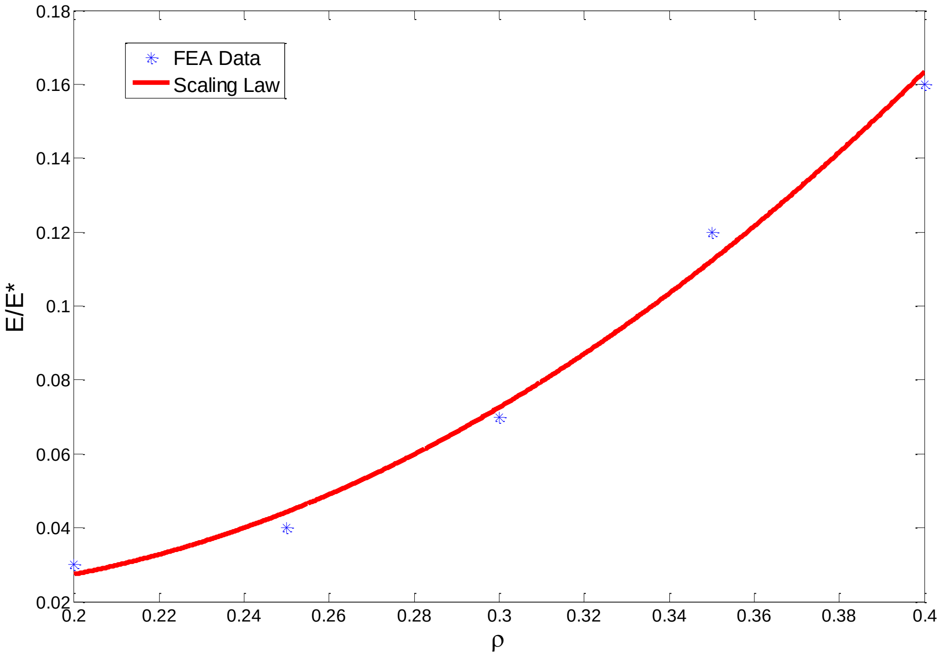

Figure 44: FEA result for relative Young's modulus

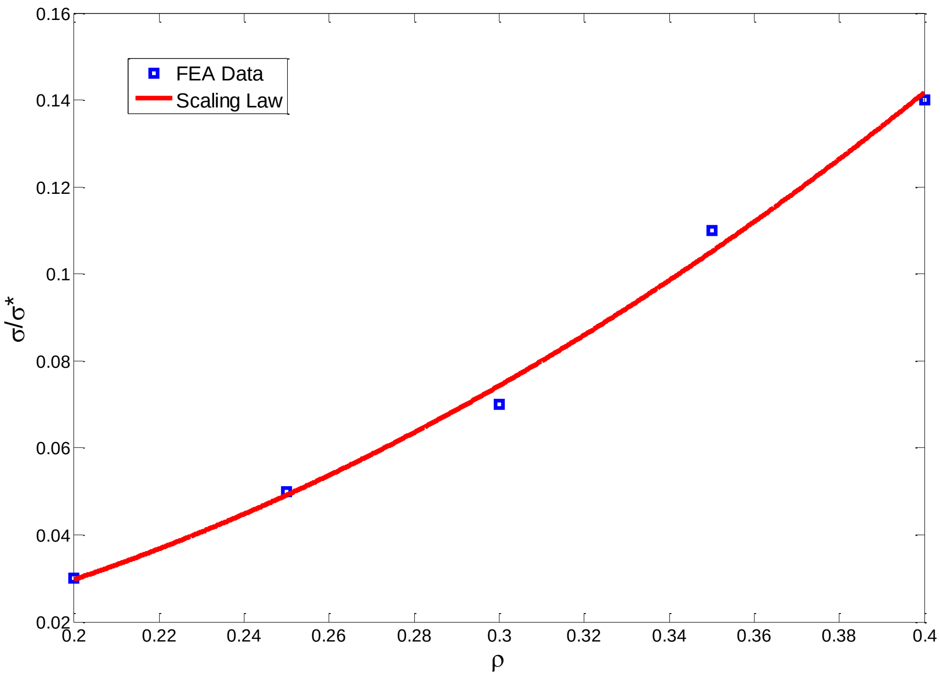

Figure 45: FEA result for relative yield strength

4. DISCUSSION AND CONCLUSION

In the thesis, five different foams with different relative density are being defined. The FE analyses are performed by the commercial FEA software. The tetrahedral mesh is the only meshing can cover whole the models. For boundary condition, which is being defined the load, comes with some converges problem, the finite element solver has better operation with displacement on boundary condition.

The comparison between the experimental result and the FE analysis, which was modeled in the FEA software for polymer foam with spherical cells yield a good estimate for Young's modulus, shown in Figure 46. The stiffness of the foams can predict with isotropic hardening and static displacement. The Young's modulus results are capable for the optimization of cellular structures. Since one of the most used functions of the cellular structure is energy absorption, which observed in some models with low porosity a notable increase of yield stress, shown in Figure 47. Exactly the models with 0.4 and 0.35 relative densities show a good value of energy absorption, which to predict the good estimate of yield stress for these models needs material modeling. As our study shows, by adding the damping factor there is a change in the plateau region. One of the reasons of this high-energy absorption may be the spherical cells, which have enough strength in low porosity the ligaments, the spherical shape increase the energy absorption, since in high porosity the ligament thickness decreases and make them unstable.

Table 5: Percent Error

Relative density	$\sigma/\sigma^{*}\ Experimental$	$\sigma/\sigma^{*}\ FEA$	Percent Error %
0.2	**0.03**	**0.03**	6.2
0.25	**0.05**	**0.05**	2.6
0.3	**0.08**	**0.07**	11.6
0.35	**0.14**	**0.10**	26.5
0.40	**0.22**	**0.13**	37.3
Relative density	$E/E*\ Experimental$	$E/E^{*}\ FEA$	Percent Error %
0.2	**0.02**	**0.03**	33
0.25	**0.04**	**0.04**	18.9
0.3	**0.07**	**0.07**	6.3
0.35	**0.13**	**0.12**	9.4
0.40	**0.18**	**0.16**	8.4

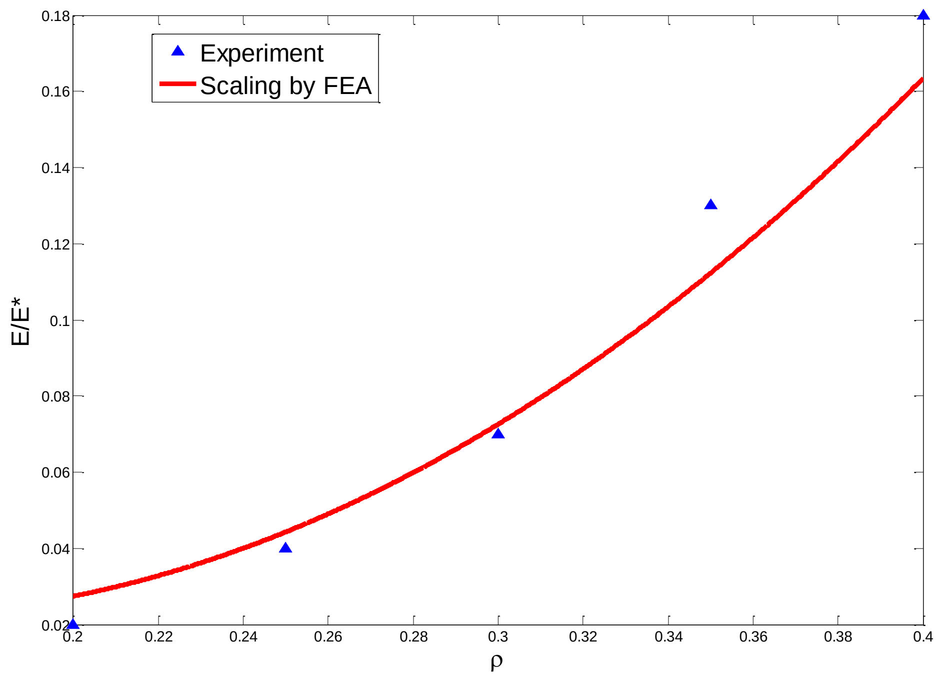

Figure 46: FEA result comparison with Experimental result for relative Young's Modulus

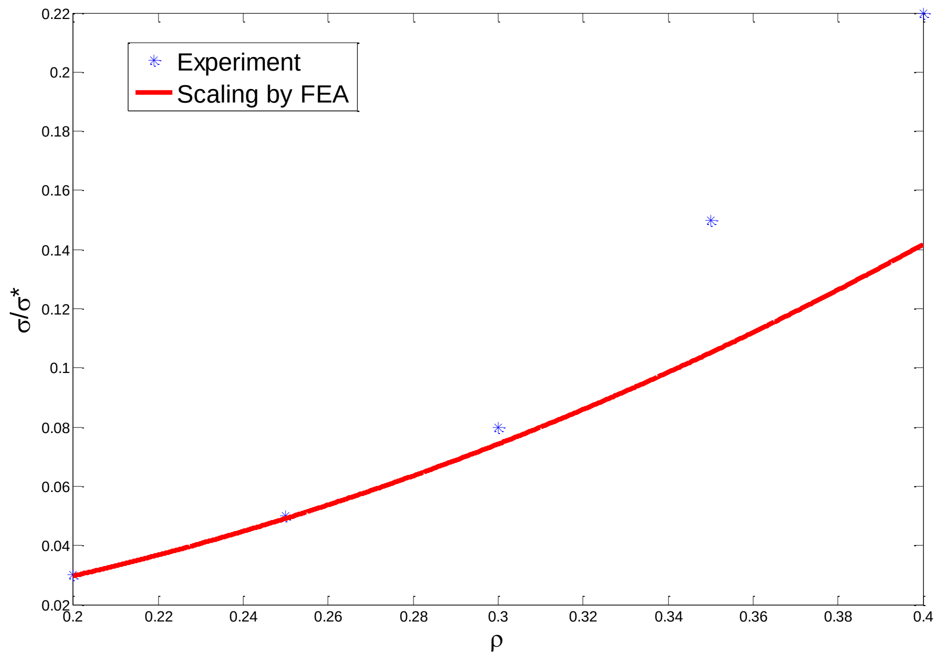

Figure 47: FEA result comparison with Experimental result for relative Yield Stress

REFERENCES

Beckmann, C., & Hohe, J. (2014). *Numerical prediction of disorder effects in solid foams using a probablistic homogenization schem.* Feriburg: Mechanics of Materials.

Bendsøe, M. P., & Sigmund. (1999). Material Interpolation Schemes in Topology Optimization. *Arch. Appl. Mech*, 635-654.

F.Ashby, M., J.Gibson, L., Evans, A., Fleck, N., Hutchinson, J., & Wadley, H. (2000). *Metal Foams: A Design Guid.* Butterworth-Heineman.

Gebhardt, A. (2012). *Understanding Additive Manufacturing.* Munchen: Carl Hanser Verlag.

Gibson, I., Rosen, D., & Stucker, B. (2010). *Additive Manufacturing Technologies: Rapid Prototyping to Direct Digital Manifacturing.* New York: Springer.

Goodall, R., & Mortensen, A. (2014). Porous Metals. In *Physical Metallurgy (Fifth Edition)* (pp. 2399-2595). Elsevier.

K, L., X, G. -L., & Subhash, G. (2005). Effects of cell shape and strut cross-sectional area variations on the elastic properties of three-dimensional open-cell foams. *Journal of the Mechanics and Physics of Solids*, 783-806.

Klahn, C., Leutenecker, B., & Meboldt, M. (2014). Design for Additive Manufacturing – Supporting the Substitution of Components in Series Products. *24th CIRP Design Conference* (pp. 138-143). Zurich,: Elsevier B.V.

Li, L., Sun, Q., Bellehumeur, C., & Gu, P. (2002). Composite modeling and analysis for fabrication of FDM prototypes with locally controlled properties. *Journal of Manufacturing Processes*, 129-141.

Michailidis, N., Stergioudi, F., Omar, H., Papadopoulos, D., & Tsipas, D. (2010). Experimental and FEM analysis of the material response of prous metals imposed to mechanical loading. *Elsevier*, 124-131.

Mun, J., Yun, B.-G., Ju, J., & Chang, B.-M. (2015). Indirect additive manufacturing based casting of a periodic 3D cellularmetal – Flow simulation of molten aluminum alloy. *Journal of Manufacturing Processes*, 28-40.

Nguyen, V.-D., & Noels, L. (2014). Computational homogenization of cellular materials. *International Journal of Solids and Structures*, 2183-2203.

Niu, B., Yan, J., & Cheng, G. (2008, November 20). Optimum structure with homogeneous optimum cellular material for maximum fundamental . pp. 115-132.

Pu Zhang, Toman, J., Yiqi Yu, Biyikli, E., Kirca, M., & Chmielus, M. (2015). Efficient Design-Optimization of Variable-Density Hexagonal Cellular Structure by Additive Manufacturing: Theory and Validation. *Journal of Manufacturing Science and Engineering*, 021004-1-8.

Ramirez, J., Cardona, M., Velez, J., & Mariaka, I. (2014). Numerical Modeling and simulation of uniaxial compression of aluminum foams using FEM and 3D-CT images. *Elsevier*, 218-222.

Szymczyk, W., & Miedzińska, D. (2010). *FEM Modeling of Failure of a Foam Single Cell.* Solid State Phenomena.

(ASTM), A. S. (2010). ASTM D638-10 STandard. *West Conshohocken,*.

J. Munguia, S. A. (2014). Compliant flexural behaviour in laser sintered nylon structures:Experimental test and Finite Element Analysis – correlation. *Materials and design*, 652-659.

Jane Chu, S. E. (2010). A comparison of synthesis methods for cellular structures with application to additive manufacturing. *Rapid Prototyping Journal*, 275-283.

Khoei, A. R. (2014). *Extended Finite Element Method: Theory and Applications.* Tehran: WILEY.

KLAUS-JURGEN, E. E. (1975). Finite element formulations for large deformation dynamic analysis. *International journal for numerical methods in engineering*, 353-389.

Michailidis, N. (2011). Strain rate dependent compression response of Ni-foam investigated by experimental and FEM simulation methods. *Materials Science and Engineering A*, 4204-4208.

N. Michailidis, F. S. (2010). FEM modeling of the response of porous Al in compression. *computational Materials Science*, 282-286.

R.K. Oruganti, A. G. (2008). FEM analysis of transverse creep in honeycomb structures. *Acta Materialia*, 726-735.

S.K. Nammi, P. M. (2010). Finite element analysis of closed-cell aluminium foam under quasi-static loading. *Material and Design*, 712-722.

S.-M. Ahn, M. M. (2002). Anisotropic material properties of fused deposition modeling ABS. *Rapid Prototyping Journal*, 248.

Michailidis, N. (2011). Strain rate dependent compression response of Ni-foam investigated by experimental and FEM simulation methods. *Materials Science and Engineering A*, 4204-4204.

Tapan Sabuwala, G. (2013). Skeleton-and-bubble model of polyether-polyurethane elastic open-cell foams for finite element analysis at large deformation. *Journal of the Mechanics and Physics of Solids*, 886-911.

Stucker, I. G. (2010). *Additive Manufacturing Technologhy Rapid Prototyping to Direct Digital Manufacturing*. New York: Springer.

Tapan Sabuwala, G. (2013). Skeleton-and-bubble mode lof polyether-polyurethane elastic open-cell foams for finite elemnt analysis at large deformation. *Journal of the Mechanics and Physics of Solds*, 886-911.

Zi-Xing Lu, Q. L.-X. (2011). Analysis of defects on the compressive behaviors of open-cell metal foams through models using the FEM. *Materials Science and Engineering A*, 285-296.

CURRICULUM VITAE

Name Surname:	Hamed Zeinalabedini
Place and Date of Birth:	
Adress:	Vişnezade Mahallesi, Zilhane Sokak no. 1 34357, Maçka, Beşiktaş, Istanbul, Turkey.
E-mail:	hamed.z.man@gmail.com

B.Sc.:	2005, Islamic Azad University, Mechanical Engineering Department
M.Sc.:	2015, ITU, Mechanical Engineering Department, Machine Design Program. The thesis accepted for **13th US national congress on computational mechanics,** California, San Diego

Teaching Experience

Dec. 2014- Mar. 2015	**Abaqus** *Freelance*
Jan. 2008- Nov. 2011	**Catia V5** *Gopath Institute, Tabriz, Iran*

Professional work experience

Jan. 2008 – Nov. 2011	**Gopath Co., Tabriz, Iran** *Design Engineer (part-time)* http://www.gopath.ir

Program skills

Catia V5	Advanced (part design, sheet metal, drift, assembly, wireframe, surface, analysis)
Abaqus	Advanced
ANSYS	Advanced
AutoCAD	Advanced
MATLAB	Advanced
Mathcad	Advanced
MS Windows	Advanced
MS Office	Advanced (Word, Excel)

Language skills

English	Fluent (speaking, writing)
Persian	Native speaker
Azerbaijani	Native speaker
Turkish	Fluent (speaking, writing)
German	Beginner

Hobbies

Mountain climbing, sports, poetry and classical music.

Reference

Name Asst. Prof. Dr. Mesut Kirca
Company ITU Faculty of Mechanical Engineering,
Mechanical Engineering Department
Email/Web site Kircam@itu.edu.tr
http://faculty.itu.edu.tr/kircam
Office Phone 0090-212 293 13 00/2572
GSM 0090 531 215 86 40

Name Asst. Prof. Dr. Erkan Günpınar
Company ITU Faculty of Mechanical Engineering,
Mechanical Engineering Department
Email/Web site Gunpinar@itu.edu.tr
http://akademi.itu.edu.tr/gunpinar/
Office Phone 0090- 212 293 13 00